AN ABSTRACT OF THE THESIS OF

Michael D. Sepp for the degree of Master of Science in Geology presented on July 13, 2016.

Title: Structural Evolution, Vein Orientation, and Paragenesis of the Botija Porphyry Cu-Mo-(Au) Deposit, Colón Panamá

Abstract approved:

_____

John H. Dilles

The Botija Cu-Mo-Au porphyry deposit is located in the Cobre Panamá mining district, which contains several deposits with a global measure and indicated and inferred resource of 14.8 MT of Cu. These deposits are associated with the Cerro Petaquilla batholith, which has U/Pb zircon ages of 26-33 Ma (Whattam et al., 2012; Baker et al., 2016). The Botija deposit is an elongate tabular body striking northeast and dipping 20-40° N and measures 2 km (length) x 1 km (width) x 600 m (height) in size. The deposit is hosted in andesite, the equigranular Petaquilla granodiorite, and a younger crowded porphyritic granodiorite with 15-50 vol.% groundmass of quartz and K-feldspar. Phenocrysts include plagioclase, hornblende ± K-feldspar and occasionally 5-15 vol.% rounded quartz eyes.

Ore is characterized by Cu-Fe sulfides (chalcopyrite > bornite) that is dominantly disseminated, but also present in magmatic-hydrothermal quartz veins. Systematic vein measurements at Botija demonstrate that copper ores are spatially associated with a quartz vein density >0.5 vol.%; these veins have two modes of structural orientation (azimuth of strike/right-hand dip) of 233/50°NW and 295/45°NE. Most similar early quartz veins are emplaced along near-vertical hydrofractures in numerous porphyry deposits globally. The present dip of these quartz veins suggest that the veins and the Botija deposit have been moderately tilted about 40° south-southeast after mineralization. Typical potassic and sericitic alteration and zonation is present in Botija, however, a late overprint of chlorite and zeolite has obscured much of the original magmatic hydrothermal alteration footprint.

Although the Botija deposit exhibits many of the common porphyry copper features, its geometry is atypical with abrupt spatial transitions (<10 m) in alteration and grades (Cu, Mo & Au) whereas most porphyry copper deposits typically exhibit gradual transitions in over hundreds of meters. These sharp breaks in the geology in some cases correspond to observed faults, and together with other faults mapped in field exposures and drill core allow identification of three main fault sets that offset the deposit. A restoration of the Cu and Mo grade shells indicates a multistage post-mineral deformation history with a first stage of ~500 m left-oblique normal offset on the Botija Fault (267/50°N) and Santa Fe fault (268/70°N), normal displacement in excess of 250 m on the NW striking Oeste fault (314/75°NE) and a final stage of normal displacement in excess of 500 m offset on S50°W-striking Strike Central faults (230/65°N). Restoration of these fault offsets brings the ore shells to the appropriate inverted cup shaped geometry typical of porphyry copper deposits. The faults identified at Botija likely accommodated

a modest amount (~10-15°) of tilting to the southeast. An additional restoration of the 50°N-dipping quartz veins to vertical restores the ore shells to geometry in line with the classical shape for a porphyry copper deposit. This restoration of quartz veins can be explained by progressive deformation initiated by presently shallowly dipping, southwest striking normal faults (240/35°NW) identified from ZTEM™ geophysics which bound the deposits of Cobre Panamá.

This reconstruction suggests the deposits of Cobre Panamá were likely dismembered by normal faulting from two or more original upright and intact porphyry copper deposits, generating the seven segmented and tilted deposits present today. This interpretation of normal displacement of the deposit is in lines with (U-Th)/He age by Farris et al. (2011), which constrain the exhumation of the deposit during a period of localized extension in Panamá between 19.5 – 22.3 Ma shortly after emplacement.

Structural Evolution, Vein Orientation, and Paragenesis of the Botija Porphyry Cu-Mo-(Au) Deposit, Colón, Panamá

By

Michael D. Sepp

A THESIS

Submitted to

Oregon State University

in partial fulfillment of
the requirements for the
degree of

Master of Science

Presented July 13, 2016

Commencement: June, 2017

Master of Science thesis of Michael D. Sepp presented on July 13, 2016

APPROVED

Major Professor, representing Geology

Dean of the College of Earth, Ocean and Atmospheric Sciences

Dean of the Graduate School

I understand my thesis will become part of the permanent collection of Oregon State University libraries. My signature below authorizes the release of my thesis to any reader upon request.

Michael D. Sepp, Author

ACKNOWLEDGEMENTS

I find myself immensely grateful to have had the opportunity to have studied under John Dilles, I am thankful for his support and mentorship through this project, during my time at OSU I have grown immensely as a geoscientist. I would also like to thank the other members of my committee Anita Grunder, Andrew Meigs, and Rene Reitsma.

I would like to thank First Quantum Minerals for their financial, technical, and logistical support for this project. I would like to thank the numerous FQM geoscientist I have worked with over the course of this project including, Sebastian Benavidez, Martin Clark, Jacinto Caberra, Ruperto Ibarra, Aurelio Fernandez, Paul Hadlum, Matt Booth, Matt Hope, and Matt Nobel. A special thanks is given to Colin Burge and Tim Ireland who through our many geological discussions have immensely contributed to the results of this project. Most importantly I would like to the geological assistants “muchachos”; without their assistance this project would not have been possible.

I would like to thank the members of the VIPER group, specifically Nansen Olsen, Federico (Fede) Cernushci, Michael Hutchinson, Jaimie Osorio, Michelle Campbell, Curtis Johnson, and Nora Utevsky for their direct assistance and multitude of geological discussion we had during my time at OSU which helped shape my research. I would also like to give a special thanks to Heather Bervid, Alaxander de Moore, and Erin Peck who assisted with the preparation of this document.

TABLE OF CONTENTS

LIST OF FIGURES

LIST OF TABLES

INTRODUCTION

The Botija deposit is located in the Cobre Panamá mining camp, operated by First Quantum Minerals (FQM), approximately 120 km west of Panamá City along the Caribbean coast (Figure 1). The district contains several porphyry copper deposits with a global measured + indicated resource of 4.2 Gt at a grade of 0.35 wt.% Cu, 6 g/t Mo, 0.07 g/t Au, and 1.3 g/t Ag at a cutoff of 0.15% Cu (Grey et al., 2015). The Mollejón low-sulfidation Au deposit is also located in the Cobre Panamá mining camp has a measured + indicated and inferred resource containing 1.37 Moz Au (Petaquilla Minerals annual report, 2013). Porphyry copper deposits have been the source of extensive academic research for over 100 years, advancing the understanding into magmatic-hydrothermal systems in arc-related subduction environments (Seedorff et al., 2005). From this vast body of research, a robust geological model for the formation of porphyry systems has been developed. The systematic zoning of alteration in porphyry copper deposits was first characterized by Lowell and Gilbert (1970), and subsequent mapping and petrological studies (Gustafson and Hunt, 1975; Dilles, 1987; Dilles and Einaudi, 1992; Proffett, 2003) have defined a genetic link between upward flowing magmatic fluids exsolved from large intermediate composition batholiths and porphyry copper deposits. This upward flowing magmatic fluid plume interacts with the wall rocks as it ascends, creating a systematic alteration from high temperature quartz vein and K-silicate stable alteration in the core of the system, zoning outward to lower temperature phyllic alteration, and zoning upward to advanced argillic alteration centered around vertically emplaced porphyry dikes which follow hydrofractures created from the upward moving fluid plume (Seedorff et al., 2005; Sillitoe, 2010; Cook et al., 2005; Weis et al. 2012).

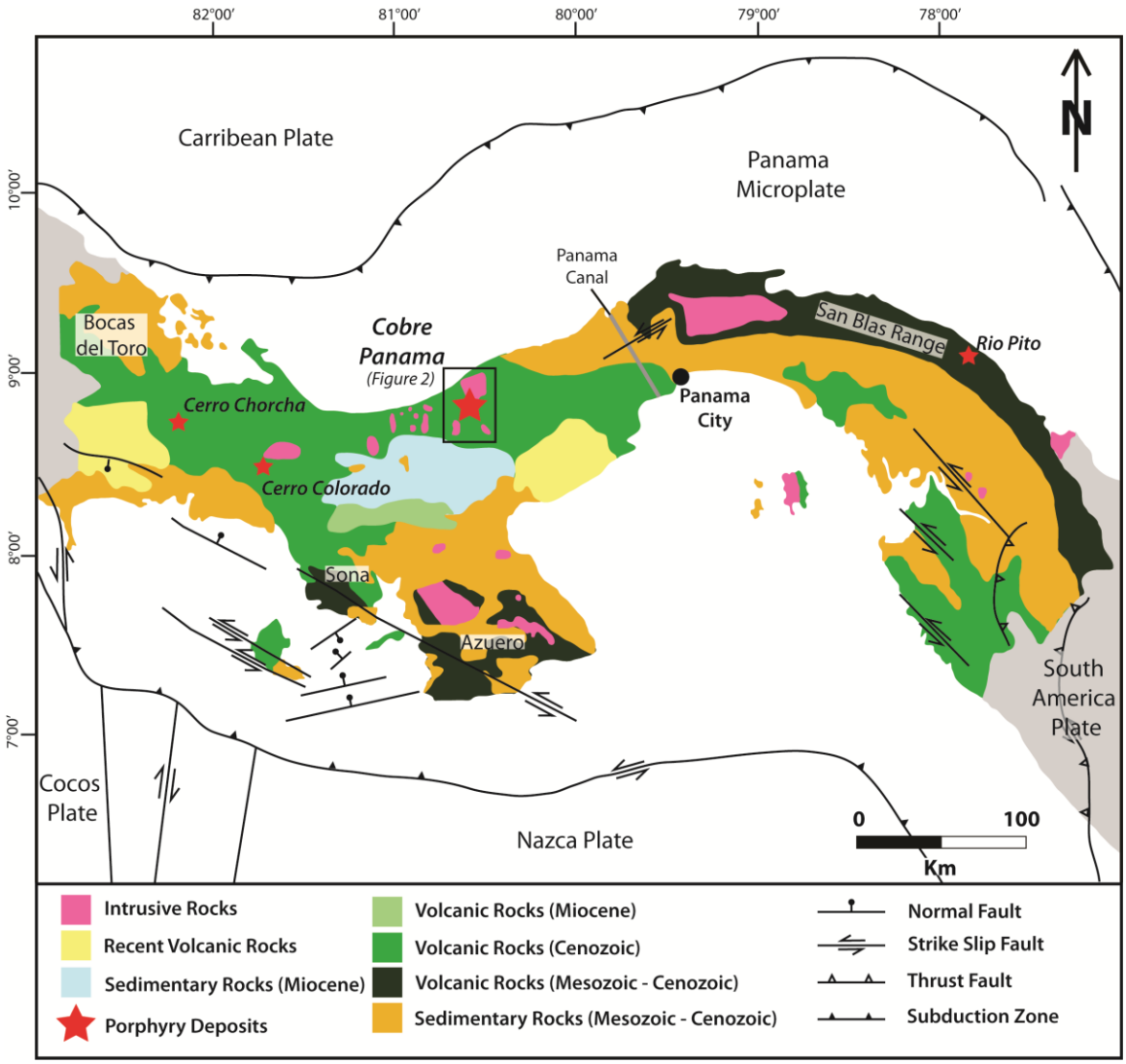

Figure 1: Simplified geologic map of Panamá with the location of discovered porphyry copper deposits, including Cobre Panamá. (After Grey et al., 2015; Whattam et al., 2012; Baker et al., 2016). Mapped Quaternary faults from Montero et al. (1998), Paris et al. (2000), Stewart and Stewart (1980), and Rockwell et al. (2010b).

The copper deposits at Cobre Panamá exhibit common attributes of a porphyry copper deposits, including the presence of porphyry dikes, quartz veins, K-silicate, and phyllic alteration, however, the geometry of the ore zones is atypical. Copper mineralization in these deposits is typically emplaced in an inverted concave shell resembling an inverted tea cup, which is centered upon vertically emplaced dike- to stock-like felsic intrusives. The vertical dimension of these

mineralized shells is one to over two times the length of the lateral dimensions (Seedorff et al., 2005). The copper porphyry mineralized shells in the Cobre Panamá mining camp have lateral dimensions which are two to three times larger than the vertical dimension, and some form flat lying bodies that dip gently 20-40° to the north/northwest. Globally, other porphyry deposits that do not exhibit the classical vertical zonation have been attributed to post-mineralization faulting/block rotation (i.e., Ann-Mason, Butte, Robinson) or differences in host rock geochemistry promoting or hindering sulfide precipitation and forming irregular ore-shell geometries (i.e. Bingham Canyon, Haquira) (Dilles and Einaudi, 1992; Houston and Dilles, 2013; Seedorff et al., 1996; Gruen et al., 2010; Redmond and Einaudi, 2010; Cernuschi, 2015).

Unlike Bingham Canyon or Haquira, the Botija deposit is predominantly hosted in geochemically homogeneous granodiorite precluding the possibility of a wall-rock induced geochemical control on the geometry of the deposit. Numerous small-scale faults are observed to crosscut altered rock in drill core. Some of these faults coincide with sharp spatial transitions (<10m) in alteration and grades (Cu, Mo, Au) which is unusual for a porphyry copper deposit that typically exhibit gradual transitions over 100s meters (Seedorff et al., 2005). This study focuses on understanding the nature of these faults on the Botija deposit, which will be the first deposit to be mined in the Cobre Panamá mining camp.

The Botija deposit is a horizontally elongate flat-lying to moderately north-dipping (10-50°NW) orebody measuring 2 km (length) x 1 km (width) x 600 m (height). Because field exposures are poor and the host rocks do not include a regular stratigraphy, this study focuses on describing the nature and geometry of the hydrothermal veins, sulfide zones, and wall-rock alteration at Botija, in order to construct a model of hydrothermal alteration zonation in the

deposit. This study also seeks to understand the orientation of veins and faults present in the deposit. Both sets of data are integrated below into a geologic structural model for Botija that includes a reconstruction of the deposit. The results from this study provide insight into the larger structural geologic history of the Cobre Panamá mining camp, which is responsible for the distribution of the seven porphyry copper and one epithermal gold deposit.

GEOLOGIC SETTING

Regional Geology:

Panamá lies on the Panamá microplate located at the junction between the South American, Caribbean, Nazca, and Cocos plates (Baker et al., 2016). The stratigraphy in Panamá has been described by Montes et al. (2012) as a succession of mafic volcanic rocks and interbedded volcaniclastic sedimentary rocks, which have been intruded by mafic to intermediate composition plutonic complexes. These volcanic and intrusive rocks postdate rocks of the Caribbean large igneous province (CLIP). Studies of Panamánian basement rocks exposed at the Soná and Azuero Peninsulas by Wörner et al. (2009) and Wegner et al. (2011) demonstrate that these rocks have trace and rare earth element signatures indicating magmatism from a plume mantle source. These conclusions agree with previous studies in Central America which have shown that younger arc-related rocks are underlain by a large igneous province with a Galapagos-like geochemical signature (Gazel et al., 2009, 2011). Several ^{40}Ar-^{39}Ar ages constrain the formation of the CLIP to 139-69 Ma (Hoernle et al., 2004; Loewen et al., 2013). Post-formation, the CLIP migrated north-northeast towards its present day position (Kerr and Tarney, 2005). The CLIP collided with the Greater Antilles arc system at approximately 70 Ma causing

subduction along the arc system to lock up and jump to the western end of the CLIP (Burke et al., 1978; Hoernle et al., 2002; Kerr and Tarney, 2005).

Two major phases of arc magmatism occurred along the western margin of the CLIP in Panamá (Whattam et al., 2012). The earlier phase has ages of 68-40 Ma (Wengner et al, 2011) and forms the early Cordillera de Panamá (Baker et al., 2016). Montes et al. (2012) identified an intermediary period between 38-28 Ma when arc-related magmatism ceased east of the Panamá Canal, however, magmatism continued west of the canal basin during this time (Whattam et al., 2012; Drummond et al., 1995). Magmatism restarted east of the Canal basin after 25 Ma, forming the modern Cordillera de Panamá between 25.4-6.8 Ma (Wegner et al., 2011; Farris et al., 2011; Rooney et al., 2011; Montes et al., 2012). Arc-related magmatism ceased in Panamá at approximately 5 Ma due to the collision of the Cocos Ridge with the subduction zone along the southwestern margin of the Caribbean Plate (Baker et al., 2016).

The isthmus of Panamá has had a complicated and long-lived deformation history owing to its location at the intersection of four plates. Left-lateral offset of the early volcanic arcs of the Cordillera de Panamá began between 40-30 Ma. Greater than 200 km of offset occurred during this time separating the early Mesozoic to Cenozoic volcanic rocks of the Soná and Azuero peninsulas from the San Blans Range (Figure 1) (Lissinna, 2005). Kerr and Tarney (2005) suggested the inception of left-lateral offset of the volcanic arcs was related to the collision of another oceanic plateau similar to the CLIP, termed the Gorgona oceanic plateau, into South America. This collision generated an anti-clockwise rotation of this isthmus of Panamá. Geodetic measurements have shown this anti-clockwise rotation of Panamá continues today (Bennett et al., 2014; Trendkam et al., 2002). This rotation is responsible for active northeast and northwest

striking sinistral faults in the eastern and southern regions of Panamá (Rockwell et al., 2010a; Rockwell et al., 2010b). Despite the predominate strike-slip motion across Panamá, Farris et al. (2011) argued for a change switch to extension in some regions of Panamá based on a change from hydrous hornblende-bearing magmatism to anhydrous hornblende-deficient volcanism between 23 to 25 Ma in the Panamá Canal Zone and Bocas del Toro (Figure 1). Low-temperature thermochronology of batholiths across Panamá, including at Cobre Panamá, and into South America indicate that exhumation of these batholiths occurred concurrent with this switch in magmatism in the Canal Zone (Farris et al., 2011). Localized zones of arc-perpendicular extension in Panamá along the Canal Zone and the Panamá-Costa Rica border could be explained as a response to formation of the oroclinal bending in Panamá and consequent generation of zones where extensional forces locally dominate (Silver et al., 1990; Farris et al, 2011). An alternative theory (Whattam et al., 2012) proposes slab rollback and tearing of the slab during this time along the western subduction margin of the CLIP was responsible for extension.

District Geology:

Seven porphyry deposits comprise the Cobre Panamá mining camp: Botija, Colina, Valle Grande, Balboa, Medio, Botija-Abajo, and Brazo. In addition, there is one low-sulfidation epithermal Au deposit, Mollejón. Additional Cu and Au prospects are also present within the district. The deposits generally form in two NW trends, one including Colina, Valle Grande, Balboa, and Mollejón; and one containing Botija, Botija-Abajo, and Brazo (Figure 2). These deposits occur along the southern margin of the NW-SE elongate Petaquilla batholith that is exposed over an area approximately 20 x 5-10 km footprint. The batholith is dominantly composed of equigranular granodiorite usually containing plagioclase (45 vol.%), quartz (30

vol.%), potassium feldspar (15 vol.%), and hornblende (10-15 vol.%). Andesitic mafic enclaves are commonly present in the equigranular granodiorite throughout the batholith (Whattam et al., 2012; Baker et al., 2016; Kessler et al., 1977). Large gabbroic to dioritic intrusions exist at the northern flank of the Petaquilla batholith near the Caribbean coast (Nobel and Benavides, 2014). Kesler et al. (1977) obtained K-Ar ages for the Petaquilla Batholith between 36.41 ± 2.06 Ma and 28.98 ± 0.35 Ma on hornblende and feldspar respectively. Whattam et al. (2012) obtained U-Pb ages on zircon between 29.0 ± 0.4 Ma and 26.1 ± 0.8 Ma from the southern end of the batholith north of the porphyry copper deposits. More recently, Baker et al. (2016) obtained U-Pb ages on zircon from a transect across the batholith and found that ages range from as old as 32.2 ± 0.76 Ma in the northern end of the batholith to as young as 27.48 ± 0.68 Ma in intrusive rocks proximal to the Colina and Balboa deposits (Figure 2). These studies indicate magmatism responsible for the Petaquilla batholith occurred over a 4 m.y. period of between 32 and 28 Ma. This age range indicates that magmatism at the Cobre Panamá mining camp occurred towards the end of the intermediary stage of arc volcanism in Panamá between 38 and 28 Ma (Montes et al., 2012) (Figure 1).

The Cu and Au deposits in the district are related to porphyritic intrusive bodies that are geochemically similar to the Petaquilla batholith but distinctly cluster along the southern flank of the batholith (Speidel et al., 2001; Baker et al., 2016; Grey et al., 2015). Variability between porphyritic rocks can be broadly divided into two groups, coarsely porphyritic rocks with crowded phenocrysts and strongly porphyritic hypabyssal intrusions aplitic groundmass, a characteristic feature of ore-related dikes in many porphyry deposits (Seedorff et al., 2005). The majority of intrusive rocks at Botija, Colina, and Valle Grande consist of coarsely crowded porphyritic

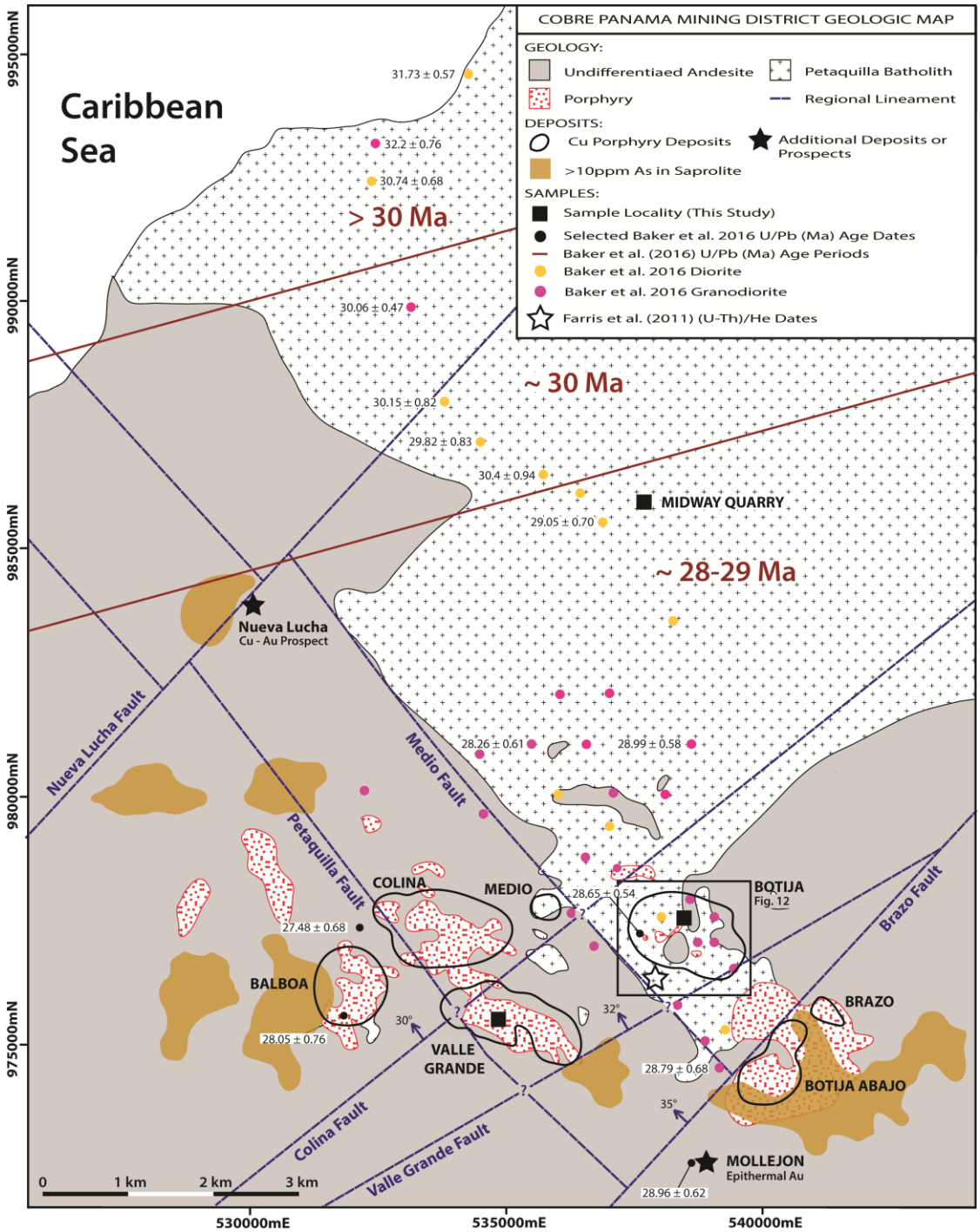

Figure 2: Simplified geological map of the Cobra Panamá mining camp, modified from Baker et al. (2016) after Speidel et al. (2001). Black lines mark the ultimate pit limits for the seven porphyry copper deposits in the district. Selected U/Pb zircon ages and geochemical samples of equiangular intrusive rocks from Baker et al. (2016) are presented in addition to the location of samples collected for (U-Th)/He fission track dates from Farris et al. (2011). Major divisions in ages of intrusive rocks of the Petaquilla Batholith are shown in red. Diorite and granodiorite composition defined by whole rock geochemistry from samples collected by Baker et al. (2016) are plotted as orange and yellow dots respectively. Zones of >10 ppm As from grid soil sampling through the district is shown in brown. Regional faults identified from aerial magnetics and LIDAR are shown in blue.

granodiorites, which are petrologically similar to the porphyritic phases within the Petaquilla batholith. These rocks generally contain 65-80 vol.% phenocrysts (60 vol.% plagioclase, 0-10 vol.% hornblende, and ~5-10 vol.% quartz eyes) and 20-35% fine-grained quartz and alkali feldspar groundmass. Due to their crowded nature, these rocks are often difficult to differentiate from the equigranular batholith in hand sample, particularly in strongly hydrothermally altered intervals. More traditional porphyry dikes typically contain 40-50 vol.% phenocrysts (plagioclase 20-30 vol.%, hornblende 0-10 vol.%, and quartz eyes ~10 vol.%) with a fine-grained aplitic quartz and alkali feldspar groundmass. These groundmass-abundant intrusives are present at all deposits but dominate intrusive types at Balboa, Botija-Abajo, and Brazo, whereas in Botija they are seldom observed.

Post-mineral andesite to basaltic andesite dikes are minor but present in the porphyry Cu deposits and extend into the batholith. These late dikes are often non-hydrothermally altered and cross-cut magmatic-hydrothermal alteration and mineralization are (Speidel et al., 2001; Speidel and Faure, 1996; Baker et al., 2016). Two $^{40}Ar/^{39}Ar$ dates from a post-mineral diorite and a post-mineral andesite dike of 30.1 ± 0.4 Ma and 28.6 ± 0.4 Ma, respectively, were obtained by Villeneuve (1997).

Speidel et al. (2001) characterized the host rocks to the Petaquilla Batholith as a series of massive to porphyritic andesite lavas, brecciated andesites, and lesser epiclastic rocks. Recent trace element soil geochemistry indicates the host rocks have a large range in the composition from andesite to komatiitic basalt with the majority of samples plotting compositionally as basalt. Recent surface exposures during mill construction in 2014 indicate subvolcanic dikes and volcanic rocks comprise the host rock succession to the felsic magmatism of the Petaquilla Batholith

(Halley, 2014; Nobel and Benavides, 2013). Age estimates from benthic foraminifera in thin interbeds of limestone within the andesite sequence indicate a middle Eocene to late Eocene age for the host rocks (Bryan, 2013), slightly predating the Petaquilla batholith.

The Cobre Panamá mining camp is covered by a thick (5-50 m) soil profile formed due to the wet tropical climate of the area. This soil profile consists of an uppermost thin humus layer typically less than one-meter-thick which is underlain by oxidized, textureless to mottled clay-limonite latosols, grading downward to saprolite which gradually increases in competency and preservation of original textures with depth (Speidel et al., 2001). This thick soil profile prevents detailed examination and geologic mapping of contacts of both the intrusive and volcanic host rocks except in drill core, drill sites, or mine infrastructure development sites, however, saprolite exposures that preserve rock textures are useful for the study of hydrothermal veins, alteration, and to a lesser degree rock types.

Porphyry mineralization in the Cobre Panamá mining camp is associated with classical porphyry Cu alteration first described by Lowell and Guilbert (1970) and Gustafson and Hunt (1975), with strong phyllic alteration near surface and laterally distal to a to a K-silicate altered core with A-type quartz veins at depth in Colina, Valle Grande, and Botija (Speidel and Faure, 1996; Speidel et al., 2001). A pervasive silica-chlorite alteration was also identified as occurring from the Botija deposit into the batholith by Speidel and Faure (2001), who interpreted this to be a background alteration of the area. $^{40}Ar/^{39}Ar$ dates from hydrothermal biotite in the K-silicate alteration zone of the Colina deposit give an estimation of the age of mineralization to 31.4 ± 0.3 Ma (Villeneuve, 1997). This age is older than many of the ages obtained by Baker et al. (2016) on felsic intrusive rocks of the Petaquilla batholith, with most samples from the porphyry deposits

dated between 28 and 29 Ma. Due to the low number of syn to post-mineral age dates the exact timing of mineralization is currently poorly constrained, but appears to have been synchronous with the magmatism of the Petaquilla Batholith.

Due to the dense tropical vegetation and well developed soil profile, the identification of major faults, their kinematics, and their relation to Cu and Au deposits has been poorly understood and is an active topic of debate today. Early exploration geologic models in the 1970s interpreted northeast- and northwest-striking faults through the deposits as conjugate sets of strike-slip faults that resulted from north-south compression, north-south structures as tensional fractures, and post-intrusion east-west striking structures as normal faults in the district (Speidel et al., 2001). Renewed geological investigation in the 1990s by Inmet Mining using newly collected satellite and radar imagery found that northwest, northeast, and north-south fault orientations dominate drainage orientations, and furthermore interpreted that major drainages followed regional scale faults and fractures (Speidel et al., 1996; Speidel et al., 2001). Geological mapping and logging of drill core identified numerous south-southeast and southwest striking, low angle fault zones (generally 20-50° dips) at Colina. Faults at Botija generally dipped steeper (generally 50-70°) with the majority striking southwest with some striking west and northwest (Speidel and Faure, 1996; Speidel et al., 2001). More recent mapping by Nobel and Benavides (2013; 2014) confirmed the presence of early moderately dipping east-west to northeast-southwest striking faults that cut and offset mineralized veins. Kinematic indicators identified in the field and drill core indicate reverse movement to local normal movement on these structures. Nobel and Benavides (2013) also interpreted the presence of a second generation of northeast- and northwest-striking, steeply dipping strike-slip faults. Whereas Nobel and Benavides (2013;

2014) attributed the majority of deformation to strike-slip and thrust faulting, they did find evidence for late normal fault on east-west and northeast striking structures which post-date and cut earlier thrust and strike-slip faults. These results conflicted with interpretations from different studies and help to demonstrate the complexity of structure in the district, which has likely seen multiple episodes of deformation.

METHODS

Diamond drill core (HQ3 and BQ) was logged at scale of 1:250 on three cross-sections, two north-south and one east-west. Cross sections are constructed in UTM 17N coordinates, with all depths/levels referenced from sea level. In total approximately. 8,000 m of core was logged with an emphasis on structure and hydrothermal features. Alteration minerals and sulfide proportions were mapped using a hand lens, with particular emphasis to note alteration minerals occupying plagioclase and hornblende sites (modified Anaconda method; see Einaudi, 1997). Assemblages were confirmed or modified by transmitted and reflected light microscope study of 85 thin sections. Mineral abbreviations are given in Table 1.

Structural logging was conducted for the entire length of a drill hole. Vein type, alteration type/intensity, and sulfide type/vol.% was logged ever 10 m in drill core. The number of quartz and D veins and their apparent width were measured over three meter intervals every 10 m to give an estimation of volume percent of both vein types. Quartz vein measurements were only of vein fill whereas D vein measurements included the vein and selvage material. Data compiled and plotted downhole and manually contoured on paper sections.

Four oriented drill holes were logged as part of this program. Core orientation was done with a spear orientation tool and hole orientation was measured with a Reflex™ gyro collected at 10 m stations downhole after drilling was completed by FQM drilling technicians. The quality of core orientation using a spear tool is heavily impacted by operator skill and core competency (Rutter, 2011). Since core competency was generally moderately to heavily fractured and operator error could not be quantified, individual measurements were treated with suspicion. Only geological features where large datasets of measurements could be collected were used in the study so that statistical significance of trends could be assessed. Additionally, vein orientations identified from drill core were compared against surficial measurements obtained near drill hole locations to access accuracy of drill hole measurements. Lithological, structural, and hydrothermal features were measured in drill core relative to the downhole orientation mark and converted to dip/dip direction. Due to the densely vegetated tropical environment and deeply weathered saprolite profile, field exposure a poor at the project site and mapping was restricted to exposures related to mine construction. Approximately 550 m of saprolite trenches and quarry benches were mapped at 1:50 and 1:100 scales. Mapping focused on recording the orientation (strike/dip), density, and mineralogy of veins in surface exposures.

Whole rock geochemistry on 26 representative lithological samples of igneous and host volcanic rocks were sent to ALS in Reno, Nevada for analysis. Samples were selected from the least altered portions of drill core and bench exposures, with great care taken to minimize chlorite and sericite alteration, which is ubiquitous through most of the drill cores. In total, 20 samples were collected from Botija, five samples were collected from Midway Quarry in the Petaquilla batholith, and one sample was collected from Valle Grande (Figure 2). Samples were

analyzed using the ME-MS61L technique utilizing a four acid (hydrofluoric-nitric-perchloric-hydrochloric) digestion and ICP-MS/AES finish. The samples were also analyzed by the ME-XRF26 method in order to obtain SiO_2 values which is not possible in the ME-MS61L method due to the formation of SiF_4 gas during sample digestion (Halley et al., 2015).

The existing FQM geological, geotechnical, and geochemical database was utilized in this study. In total, 538 drill holes have been drilled at Botija with a nominal grid spacing of 100 m, amounting to 108,900 m. Drill core was half cut and sampled with an average downhole width of 1.5 m per sample over the entirety of every drill hole. Samples were sent for geochemical determination at ALS in Lima, Peru using ICP-MS. Digestion of the samples was done either by 4 acid or aqua regia digestion. Aqua regia digestion utilizes hydrochloric and nitric acids, which is useful in the determination of many base and precious metals, however, this digestion technique has limited effect in the dissolution of silicate minerals (Rutter, 2011; Halley et al., 2015). Due to mixed dataset of digestion techniques, only elements concentrated into sulfides and sulfates (i.e. Cu, Au, Mo, As, Se, Te, Sn, Tl, Ni, and Zn) were used in the study. A soil geochemistry grid was also collected across the mining camp on a 500 m grid. Soil samples were analyzed with a four acid digestion with ICP-MS finish to allow determination of hydrothermal trace elements to map the footprint of the porphyry systems.

Geological logging and orientation data and assay results were imported into Leapfrog Geo v. 3.1 and used to develop a three-dimensional geologic model of the Botija deposit. Leapfrog Geo uses implicit modeling to generate three dimensional models of numeric and geologic data using radial basis function (Carr et al., 2001; Stewart et al., 2014). This method of implicit modeling was first introduced into the geosciences by Hardy (1971) for interpolation of irregularly scattered

topographic data but has become popular for interpretation of numeric and recently geologic data in mining and mineral exploration due to the speed of interpolation in implicit modeling vs traditional two dimensional geologic wireframing (Cowan et al., 2002; Birch, 2014). Identified faults were used in Leapfrog and used to constrain the three-dimensional model of copper, molybdenum, and gold mineralization at Botija.

Table 1. Mineralogical Abbreviations

Act	Actinolite	Cu-Ox	Copper oxide	Ksp	K-feldspar	Geo	Goethite
Anh	Anhydrite	Cp	Chalcopyrite	Mb	Molybdenite	Mn-Ox	Manganese oxide
Bi	Biotite	Ep	Epidote	Mt	Magnetite	SC	Shreddy Chlorite
Bn	Bornite	Gyp	Gypsum	Musc	Muscovite	Ser	Sericite
Cal	Calcite	Hbl	Hornblende	Plag	Plagioclase	Zeo	Zeolite
Carb	Carbonate	Hem	Hematite	Px	Pyroxene		
Cc	Chalcocite	Jar	Jarosite	Py	Pyrite		
Chl	Chlorite	Kaol	Kaolinite	Qz	Quartz		

GEOLOGY

Host Rocks:

Extrusive volcanic and subvolcanic intrusions of the host andesite package are present to the north and northeast of the Botija deposit. These andesites are notably barren of mineralization, however, a mineralized andesite package is present in the Center of the Botija deposit (Figure 2). Copper grades and hydrothermal alteration in this andesite package is notably less than the immediately in adjacent felsic intrusives. Mineralization is strongly fracture-controlled within the andesite package, whereas, sulfide mineralization in the felsic intrusives is mostly disseminated. Lateral contacts of this andesite package are fault bounded along the western and eastern flanks of the package, while the contacts at the bottom of the andesite package against the felsic plutonic rocks are intrusive.

Four intrusive rocks types are present at the Botija deposit; a summary of key identifiable features is presented in Table 2. The Petaquilla granodiorite and the Late Porphyries constitute textural end members of equigranular and porphyritic rocks at Botija. The Petaquilla granodiorite, as observed at Botija, is compositionally and mineralogically similar to rocks of the Petaquilla batholith described in previous studies (Whattam et al., 2012; Baker et al., 2016; Kessler et al., 1977). The Petaquilla granodiorite is a medium-grained (0.25 – 4 mm) equigranular granodiorite with quartz and K-feldspar intergrown between interlocking plagioclase and hornblende crystals. The Late Porphyries are strongly porphyritic rocks (50-75 vol.% groundmass) with medium-grained (0.25 – 4mm) plagioclase, hornblende, and resorbed 'quartz eye' phenocrysts in a fine-grained (0.03 – 0.1 mm) groundmass consisting of quartz + K-feldspar.

Table 2. Key Petrologic Features of Botija Intrusive Rocks

		Phenocrysts vol% and Grain Size								
	Rock Texture	Ksp	Plag	Hbl	Qz	Bi	Px	Qz Texture	Pheno vol%	GM vol% & Grain Size
Petaquilla Granodiorite	Eq	0-15% 0.5-4mm	60-67% 0.5-3mm	5-12% 0.2-2mm	15-25% 0.2-2mm	tc		I		
Transitional Porphyry	Seri	tc	40-75% 0.25-4mm	5-15% 0.2-3.5mm	5-15% 0.25-3mm			R & I	50-85%	15-50% 0.1-0.5mm
Late Porphyry	Ppy		30-50% 0.25-3mm	3-10% 0.25-3mm	5-15% 0.25-4mm			R	30-50%	50-70% <0.03-0.1mm
Basaltic Andesite Dikes	Ppy		0-25% 0.1-3mm	tc			0-10% 0.2-3mm		5-30%	70-95% 0.03-0.5mm

Abbreviations: Pheno = Phenocryst, GM = Groundmass, Eq = Equigranular, Seri = Seriate, Ppy = Porphyritic, I = Interstitial, R = Resorbed, tc = Trace

The majority of mineralization is hosted in the transitional type porphyries which define a spectrum of porphyritic intrusions between the end member Petaquilla granodiorite and the Late Porphyries. The groundmass of the Transitional Porphyries ranges from porphyritic to seriate in texture, is coarser-grained (0.1 – 0.5 mm), and is volumetrically less abundant

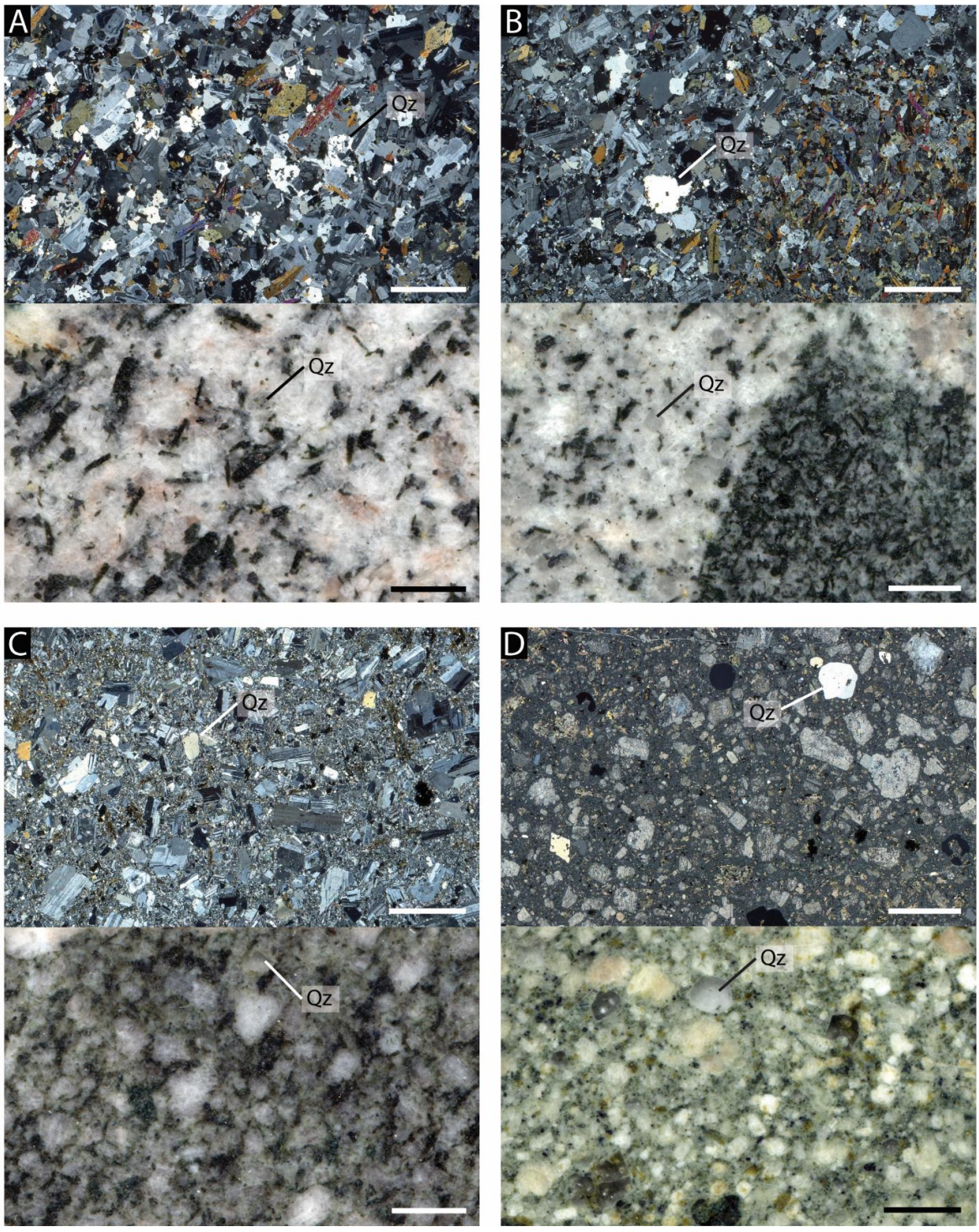

Figure 3: Examples of felsic intrusive rocks from the Botija deposit with photomicrographs taken in cross-polarized light above and rock slab photos below; scale is 0.5 mm for all photos. A. Equigranular Petaquilla granodiorite with quartz and K-feldspar interstitial to plagioclase and hornblende crystals. B. Seriate transitional porphyry with quartz crystals showing a trimodal grain size, 0.75-2mm phenocryst, and 0.05-0.03/0.3-0.75mm interstitial quartz to plagioclase and hornblende phenocrysts. A mafic enclave containing hornblende and plagioclase in disequilibrium with the seriate porphyry is located in the lower right hand side of the sample C. Crowded porphyritic transitional porphyry with subrounded quartz, plagioclase, hornblende phenocrysts in a fine-grained (0.3-0.1mm) groundmass. D. Late porphyry with rounded quartz phenocrysts, plagioclase, hornblende phenocrysts in a very fine-grained (<0.03mm) groundmass.

(15 – 50 vol.%) than the groundmass of Late Porphyries. Quartz phenocrysts occur interstitial to other minerals and are irregular to subrounded. The Transitional Porphyries occasionally have mafic enclaves, similar to the Petaquilla granodiorite, whereas the Late Porphyries do not contain mafic enclaves. The strongly crystalline nature of the Transitional Porphyry indicates these rocks experienced a longer duration of crystallization compared to the Late Porphyries, however, the Transitional Porphyries still experienced pressure quenching due to loss of volatiles (Burnham, 1979; Dilles, 1987) and quenching. Due to the lack of clear intrusive contacts and as a result of strong post-mineral alteration and deformation, further delineation of sub-units within the Transitional Porphyries cannot be made, however, the Late Porphyries appear to have post-dated the Transitional Porphyries due to the lower intensity of hydrothermal alteration and mineralization present in the Late Porphyries compared to the Transitional Porphyries.

Late mafic dikes cross cut the hydrothermally altered and mineralized rocks at Botija. These dikes are mostly very fine-grained rocks but can contain minor (0-30 vol.%) plagioclase and pyroxene phenocrysts. Mafic dikes are devoid of high-temperature alteration, but occasionally have pyrite-filled fractures and propylitic (epidote ± sericite ± chlorite) alteration.

Previous geochemical studies in the Cobre Panamá mining camp have generally classified the felsic intrusive rocks associated with mineralization as granodiorites in composition (Kessler et al., 1977; Whattam et al., 2012), though these studies were limited in their scope. Baker et al. (2016) collected 196 samples across the Cobre Panamá mining camp and found the intrusive rocks of the Petaquilla batholith ranged in composition between diorite to granodiorite, porphyry samples compositionally overlapped with equigranular granodiorite samples. A trend of increasing geochemical evolution can be discerned in the rocks of the Petaquilla batholith, with

more primitive dioritic samples occurring in the northern end of the batholith (Figure 2). This separation in composition and age of the samples indicates the Petaquilla Batholith is a multiphase batholith. A negative trend in Al_2O_3, MgO, Fe_2O_3, P_2O_5, TiO_2, and V plotted against SiO_2 is observed between the dioritic samples of equigranular and porphyritic rocks collected by Baker et al. (2016) and granodioritic samples (Figure 4). This tight negative trend was used by Baker et al. (2016) to argue for fractional crystallization as the dominant process in the formation of the Petaquilla batholith. Results from samples of the Transitional Porphyry at Botija overlap and extend to higher silica contents compared to equigranular granodiorite samples from the Petaquilla Batholith.

Veins and Wall-Rock Alteration:

The sequence of magmatic hydrothermal veins at Botija evolves from early K-Silicate stable assemblages to hydrolytic and late zeolite ± calcite alteration. A paragenesis table showing this progression is presented in Figure 5. This sequence follows a classic hydrothermal alteration sequence for a porphyry copper deposit observed in numerous other deposits including El Salvador, Ann-Mason, and Bingham Canyon (Gustafson and Hunt, 1975; Dilles and Einaudi, 1992; Redmond and Einaudi, 2010). A summary of the major vein types is presented in Table 3 and photographs of the veins in Figure 6. Sericite is a ubiquitous mineral in the selvages of most of the vein types. Sericite is not a stable alteration mineral for many of the vein types it is observed with, it is interpreted the sericite was introduced during a late phyllic alteration that exploited existing veins as preferred fluid pathways.

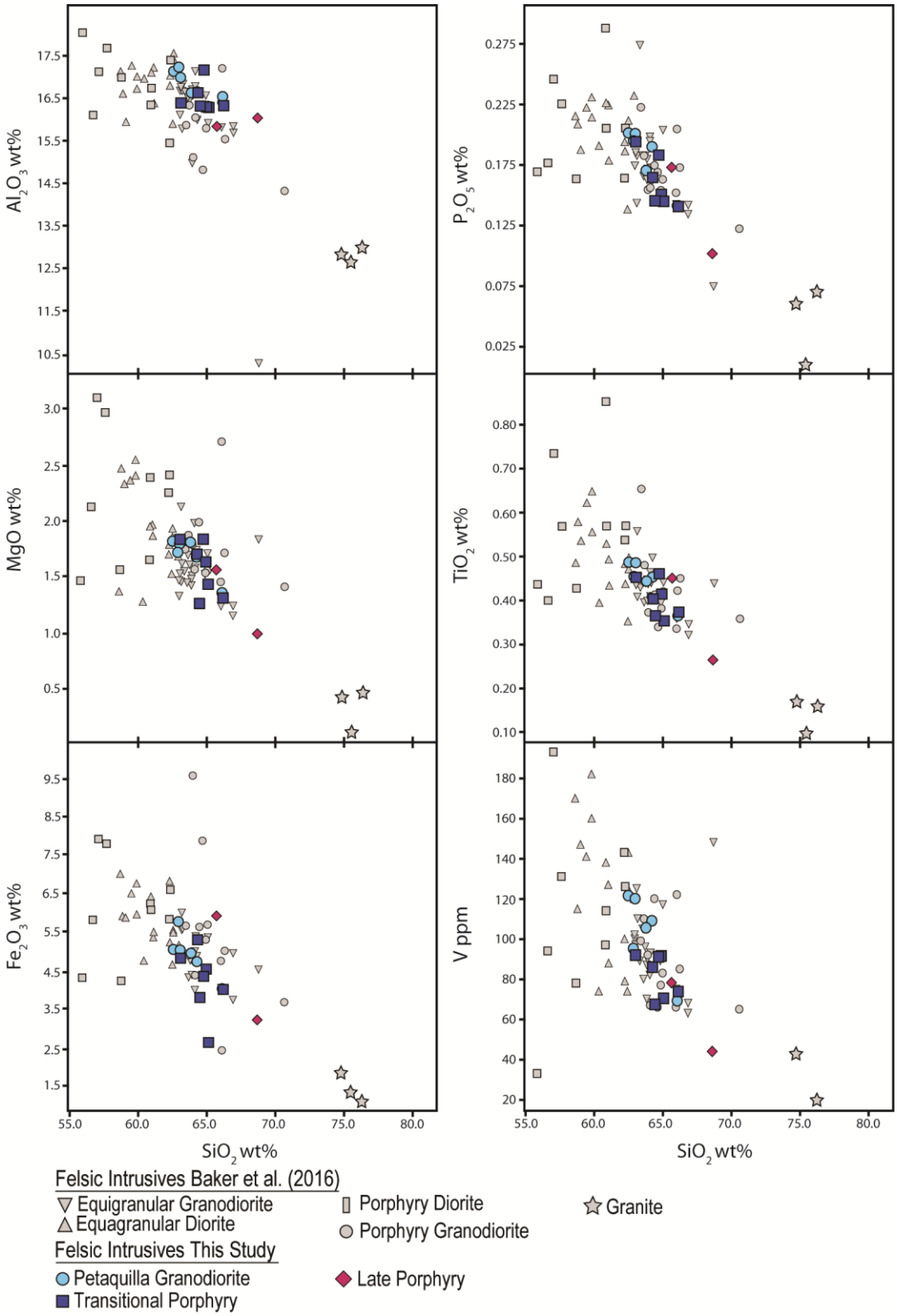

Figure 4: SiO_2 vs Al_2O_3, MgO, P_2O_5, TiO_2, Fe_2O_3, and V for felsic intrusive rocks in the Cobre Panamá mining camp, data from Baker et al. (2016) and results from this study.

Aplite Dikes: Aplites are aphanitic dikes 0.5 – 6.5 cm in width which contain equal proportions of K-feldspar and quartz. Rare chalcopyrite and pyrite are present in aplites. These sulfides appear to have been introduced with the aplite dikes but do not contribute significantly to sulfide introduction to the deposit. Aplites are rare in the core of the deposit, occurring predominantly north of the ore body or at depth to the south of the deposit. Cernuschi (2015) estimated temperature of formation for aplite dikes at Haquira at ~650°C, higher than the estimates for quartz veining (550-600°C). This interpretation is consistent with field observations at Haquira where the highest densities of aplites are present in the deepest part of the deposit (Cernuschi, 2015). These temperature estimates suggest that aplite dikes form deep in magmatic-hydrothermal systems relative to copper mineralization which is associated with quartz veins.

Biotite Veinlets: Irregular veins containing hydrothermal biotite, shreddy chlorite, and muscovite which contain chalcopyrite with variable pyrite. Chlorite is shreddy (shreddy chlorite) in texture and appears to have replaced earlier-formed hydrothermal biotite (Figure 7a). It is interpreted that the chlorite is a late alteration post-formation of the biotite veinlets. The term shreddy chlorite is used for chlorite altered hydrothermal biotite. Biotite veinlets are present in the core of the deposit, but also occur in localized sheeted sets distal to the orebody and are responsible for localized copper anomalies.

Early Dark Micaceous (EDM) Veins/Veinlets: Symmetric alteration selvages with coarse-grained sericite and shreddy chlorite on fractures. As with the early biotite veinlets, the shreddy chlorite in these veins is interpreted to represent original hydrothermal biotite which has been subsequently altered to chlorite. Selvages are sulfide rich (>1 vol.%) and contain both chalcopyrite and pyrite. These fracture-controlled selvages fall into the category of EDM halos

identified previously at depth in other porphyry copper deposits including Butte (Meyer, 1965), Bingham Canyon (Redmond and Einaudi, 2010), and Haquira (Cernuschi, 2015). Few EDM selvages were recorded in logging but were observed throughout the deposit.

Quartz veins: A and B veins, as defined by Gustafson and Hunt (1975), are present at Botija. The majority of quartz veins are transitional between these two end member quartz vein types and are termed AB veins. A-type quartz veins are generally barren quartz veins 1 – 20 mm in width which seldom contain minor pyrite ± chalcopyrite which appears along fractures within the quartz vein. A-type veins have well developed selvages of K-feldspar, shreddy chlorite, hydrothermal biotite and sericite. Anhydrite is present in A veins at depths greater than 270 m and appears to texturally replace quartz in the veins. B-type quartz veins are straight walled, range in width between 3 – 25 mm and have characteristic centerlines containing chalcopyrite and variable amount of pyrite, molybdenite, and bornite. B-type veins commonly do not have selvages but occasionally have shreddy chlorite, K-feldspar, and sericite selvages.

Transitional AB veins tend to be wavy, range in width between 0.3 – 6 mm, and are compositionally similar to B-type veins but do not have centerlines developed nor contain molybdenite. AB-type veins also generally have more well-developed shreddy chlorite, K-feldspar, and sericite selvages with disseminated sulfides present in the alteration selvage. The appearance of shreddy chlorite alteration down hole strongly correlates with the appearance of quartz veins indicating that K-silicate alteration was associated with quartz veins. Later sericite and chlorite alteration overprinted earlier K-silicate and impeded the identification of the limit of original K-silicate alteration.

Quartz crystals in the veins do not have the sugary or vuggy texture typical of magmatic-hydrothermal quartz veins. The quartz crystals show evidence for stress recrystallization (Figure 7b) causing many of the A and B type veins to lose their characteristic granular sugary or vuggy infill textures as described by Gustafson and Hunt (1975). Some veins show pseudo-mosaic textures which indicate moderate to high temperature deformation of the quartz occurred subsequent to vein formation (Davis and Reynolds, 1996). Quartz veins are also commonly vuggy with between 0 and 20 vol.% vein material dissolved indicating that either quartz or possibly anhydrite could have been dissolved by subsequent fluids.

Quartz-Molybdenite Veins/Veinlets: Quartz molybdenite veins are less common than AB and B quartz veins but contain the majority of molybdenite in the deposit. These veins contain quartz and sulfides with an overwhelming majority of sulfides occurring as molybdenite, approximately 10 – 50 vol.% of vein material. Only a minor proportion (<10%) of sulfides in these veins occurred as chalcopyrite and pyrite and were likely introduced by later fluids which reopened the quartz-molybdenite veins. Quartz-molybdenite veins do not have alteration selvages developed but occasionally have sericite selvages where the quartz-molybdenite veins had been reopened by later fluids. Quartz in these veins is observed to have a vuggy infill forming subhedral to euhedral quartz crystals, however, as with other A to B family quartz veins recrystallization of quartz and molybdenite has occurred in these veins.

Chalcopyrite Veinlets: Irregular chalcopyrite ± pyrite ± quartz fill on fractures that do not associated with alteration selvages. These veinlets typically occur in sheeted sets that range in density from scarce (>1 m spacing) to dense (1 - 100 cm) scale spacing and contribute a modest amount of copper to overall endowment where spacing is dense. The majority of chalcopyrite

Table 3. Vein Characteristics at Botija

				Vein Fill			Vein Halo		
	Vein Type	Vein Abundance	Wall Geometry	Width (mm)	Gangue	Sulfides	Width (mm)	Gangue	Sulfides
Early	Aplite (Ap)	R	Wavy	5 - 65	Ksp + Qz	± Cp ± Py[1]			
	A	R - C	Wavy	1 - 20	Qz ± Anh	± Cp ± Py[1]	1 - 8	Ksp ± SC[2] ± Bi + Ser[1]	
	Early Bi	R - C	Irregular Fracture Selvage	0.05 - 0.5	Bi + SC ± Musc	Cp ± Py	0 - 4	Bi + SC ± Musc	± Cp ± Py
Ore Stage	EDM	VR	Irregular	5 - 10				Musc + SC	Cp ± Py
	AB	C	Wavy	0.3 - 6	Qz	Cp ± Bn ± Py[1]	0 - 6	Ser[1] + Cal[3] ± SC[2] ± Ksp	Cp
	B	C	Straight Walled, Centerlines	3 - 25	Qz	Cp ± Mb ± Bn ± Py[1]	0 - 3	Ser[1] + Cal[3] ± SC[2] ± Ksp	± Cp
	Qz Molybdenite	R - C	Straight Walled	1.3 - 6	Qz ± Ser	Mb ± Cp[1] ± Py[1]		± Ser[1]	
	Cp Veinlets	C	Irregular	0.2 - 2	± Qz ± Ser[1]	Cp ± Py			
Late	D	C	Straight Walled, Commonly Sheeted Sets	0.4 - 7	Qz	Py ± Cp	0.75 - 70	Ser + Qz	Py
	Py Veinlets	R	Irregular	0.2 - 2	± Qz ± Ser[1]	Py ± Cp	0 - 2	± Ser	
	Lode Veins	VR	Straight Walled, Fault Contacts	200 - 400	Qz + Ser ± Chl ± Mt	Py ± Cp	0 - 15	± Ser ± Chl	
	Carbonate - Sulfide	VR	Straight Walled	9 - 60	Carb + Ser	Py ± Gray Sulfides	0 - 60	Ser + Carb	Ser
	Calcite Veinlets	C	Straight Walled, Irregular	<0.1 - 0.2	Cal + Gyp				
Propylitic Veins	Chlorite - Epidote	C	Irregular	0.1 - 6	Chl + Qz ± Ep ± Mt	± Py	1 - 8	Chl + Ep ± Ser	
	Epidote	R - C	Irregular	0.1 - 30	Ep + Ser + Qz	± Py ± Cp	0 - >50	Ep + Ser ± Chl	
	Actinolite	VR	Wavy	0.5 - 1	Act + Ep + Chl				

Abbreviations: Vein abundance: C = common, R = rare, VR = very rare. Veins are grouped by their relation to mineralization, Early, Ore Stage, Late and Propylitic.
[1]Possibly related to later quartz-sericite-pyrite stage alteration; [2]Shreddy chlorite appears to be a later chlorite replacement hydrothermal biotite
[3]Calcite observed in all vein types is introduced during high temperature alteration, low temperature meteoric alteration, or both

Reverse Relationship / Normal Relationship		Early				Ore Stage					Late			
		Ap	A	Early Bi	EDM	Cp (Early)	AB	B	Qtz-Mb	Cp (Late)	Py	D	Prop	Cal
Early	Ap												1	
	A	2			1	1								
	Early Bi	8	2				1							
	EDM		1											
Ore Stage	Cp (Early)	1												
	AB	1		1	2	2		1						
	B	1	1	1	2	3	8		3					
	Qtz-Mb	1	1		2	1	3	3						
	Cp (Late)	4	3	1	1	1	14	8	3					
Late	Py	2	11	4			7	3	1	2				
	D	1	5	3	1	0	3	5	7	1				
	Prop	9	7	8	1	2	6	6	1	4	7	4		
	Cal	1	5	1	1	1	8	7	4	8	4	10	9	

Figure 5: Matrix of observed vein cross cutting relationships. Veins are grouped according to their vein stage, early premineral, ore stage, and late post-mineral. Two generations of chalcopyrite veinlets are identified in the ore stage, one early and one late, Cp (Early) and Cp (Late), respectively. All propylitic vein types are grouped together (Prop).

veinlets cut quartz veins (Figure 5 Cp Late), however, a small subset of these veins are cut by quartz veins (Figure 5 Cp Early) likely indicating that multiple pulses of high-temperature hydrothermal activity lead to overprinting quartz and chalcopyrite veinlets; a commonly feature of high temperature in porphyry systems (Tosdal and Richards, 2001).

Hydrolytic alteration: Pyrite ± quartz ± sericite veins with pervasive alteration selvages of sericite-pyrite-quartz as defined by Gustafson and Hunt (1975) are present at Botija. These D veins overprint and offset previously discussed vein types. Pyrite veins with poorly to unformed selvages were classified as pyrite veinlets but were only locally present in the deposit. These pyrite veinlets are interpreted to have formed when water to wall rock ratios were lower than for the formation of classic D veins. Tan (Figure 7c) and green (Figure 7e) sericite alteration of

feldspar crystals is present throughout the deposit, but is primarily focused in the western portion of the deposit. The intensity of this alteration does not correlate with the density of D veins. Alteration varies from a light dusting to complete replacement of feldspar crystals and is associated with pyrite ± chlorite alteration of mafic sites. Hyperspectral imaging indicates the tan sericite is illitic in composition. The pale green sericite is likely phengitic (Halley et al. 2015). Sericite alteration associated with D veins tends to be grey to white in color, and coarser grained (~0.1 mm) than the tan and green sericites (<0.05 mm). Fractures with tan sericite fill (Figure 7g) crosscut earlier hydrothermal veins/alteration including D veins, indicating that tan sericite alteration postdates higher temperature phyllic alteration associated with D veins. Strong sericite alteration of the wall rock is typically accompanied by an increase in disseminated quartz throughout the wall rock. An increase in disseminated quartz crystals throughout the wall rock is associated with sericite alteration and is generated from liberated SiO_2 from the hydrolytic reaction of feldspar converting to sericite (Meyer and Hemley, 1967; Pirajno, 2009). The presence of D veins and tan sericite alteration of the wall rock is most intense (2-20 vol.% D veins and 30-80% of feldspar crystals replaced by sericite) and principally found above the area of highest density of quartz veins and copper mineralization but locally penetrated into the core of the orebody where it cross-cuts A-B veins associated with most copper mineralization.

Lode Veins: Lode veins are not common in the Botija deposit, although they occur more abundantly in the far western and eastern portions of the deposit. Lode veins mostly contain pyrite ± chalcopyrite ± magnetite, are much larger than other vein types, 50 – 400 mm in width, and have fault-bounded contacts with clay gouge zones. The presence of these veins is associated with elevated concentrations of tellurium, bismuth, arsenic, and silver when compared to

surrounding and older K-silicate and sericitic altered wall rock. Enrichment in these elements indicates formation in higher levels of the magmatic hydrothermal system (Halley et al. 2015). In addition to these quartz-sulfide veins, carbonate-sulfide ± sericite veins are present in Botija, these veins range in apparent width between 9 – 60 mm. Pyrite constitutes the majority of sulfides (>95%) with minor fine-grained but unknown grey sulfides. These veins differ from the quartz-sulfide veins in the strong development of sericite + carbonate selvages and diffuse, non-faulted contacts.

Disseminated and fracture-controlled anhydrite alteration is occasionally observed at depth below zones containing gypsum (the gypsum front) similar to hydrothermal anhydrite at El Salvador described by Gustafson and Hunt (1975). Fracture-controlled anhydrite is older than earlier anhydrite with quartz veins, overprinting quartz veins, and lode veins, but predates late hydrolytic alteration.

Propylitic Alteration and Veins: Veins containing chlorite + quartz ± pyrite and epidote + sericite + quartz are present in the deposit. Little propylitic alteration is present in the core of the deposit, occurring mostly distal to the copper orebody. Whereas the majority of mafic dikes did not contain hydrothermal alteration, some mafic dikes contain propylitic veins containing epidote and chalcopyrite, supporting the notion that at least some of the mafic dikes were already emplaced towards at the end of the hydrothermal activity.

Post-Magmatic-Hydrothermal Alteration and Veins: Late fractures and faults which cut the magmatic-hydrothermal veins/alteration and propylitic alteration are commonly filled by zeolite + chlorite ± calcite. The spatial variation of this fault-related zeolite alteration will be discussed

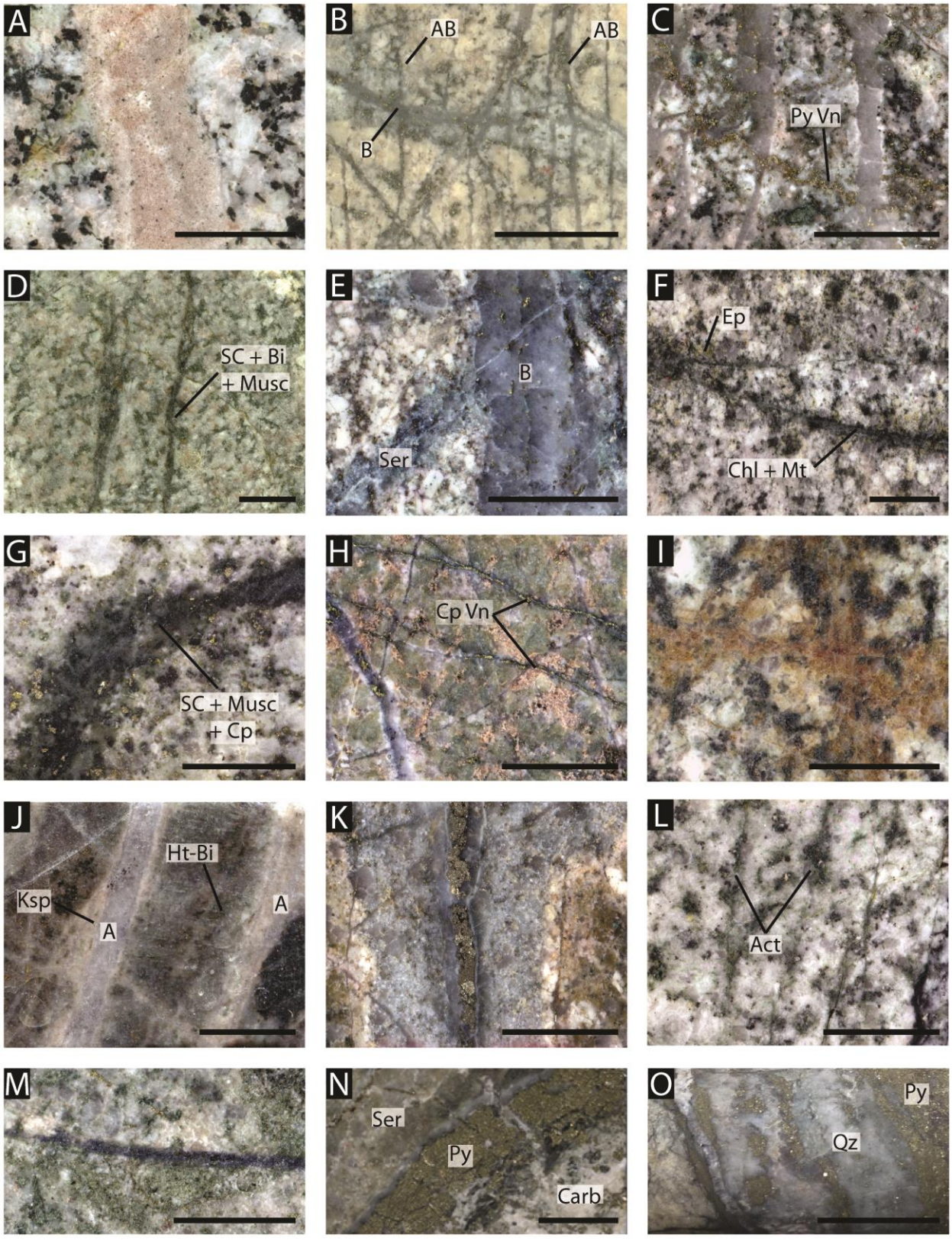
A
B
AB
AB
B
C
Py Vn
D
SC + Bi
+ Musc
E
B
Ser
F
Ep
Chl + Mt
G
SC + Musc
+ Cp
H
Cp Vn
I
J
Ht-Bi
Ksp
A
A
K
L
Act
M
N
Ser
Py
Carb
O
Py
Qz

Figure 6: Photographs of veins and age relationships between veins, scale is 1 cm for all photos. A. Aplite dike intruding equigranular granodiorite. B. Vertically sheeted AB quartz veins cross cut by a B quartz vein. C. Wavy pyrite veinlet cross cutting B quartz veins. D. Early biotite veins containing abundant shreddy chlorite, muscovite, and chalcopyrite. E. Large B quartz vein with well-developed centerline infilled with chalcopyrite. B quartz vein is crosscut by fracture with sericite selvage. F. Chlorite-magnetite vein with patchy epidote selvage. G. Wavy EDM vein containing shreddy chlorite, muscovite and >1 vol.% chalcopyrite. H. B quartz vein (left side of photo) is crosscut by chalcopyrite veinlets. I. Irregular epidote veins with sericite, epidote, and chlorite alteration selvages. J. Stockwork barren A quartz veins with hydrothermal K-feldspar and biotite selvages on larger veins. K. D vein with pyrite + quartz vein fill with pervasive white sericite + quartz + pyrite alteration selvage (grey envelope) transitioning out to non-texturally destructive partial tan sericite + pyrite alteration. L. Irregular sheeted actinolite veinlets. M. Quartz molybdenite vein. N. Carbonate-pyrite vein with texturally destructive sericite alteration selvage. O. Quartz-pyrite lode vein with sharp wall rock contact (left side of photo). Lode vein does not have a clear alteration selvage.

below. Chlorite appears to have been introduced in two stages, during propylitic and zeolite alteration. The timing of chlorite alteration provides a genetic constraint for the silica-chlorite alteration identified by Speidel and Faure (1996). The chlorite in this assemblage is attributed to these two chlorite alteration events, the silica is attributed to silica formed as a result of sericite alteration of feldspar crystals during phyllic alteration. The silica-chlorite is therefore an amalgamation of both phyllic and post magmatic-hydrothermal alteration, postdating the introduction of copper mineralization.

Magmatic-hydrothermal veins and alteration are also crosscut by gypsum and calcite veinlets. Calcite alteration of plagioclase crystals is present throughout the deposits. It is unclear whether this calcite alteration is related to high-temperature magmatic-hydrothermal alteration, low temperature meteoric alteration, or both. Below depths of 300 m late millimeter to centimeter scale gypsum veins cross cut earlier vein types. The presence of these veins below this depth is associated with an increase in rock competency. These gypsum veins were likely formed as a result of dissolution of anhydrite by post-magmatic meteoric fluids which precipitated gypsum at greater depth along fractures. Anhydrite is also present below depths of 300m, increasing in abundance with depth. This process of anhydrite dissolution by meteoric

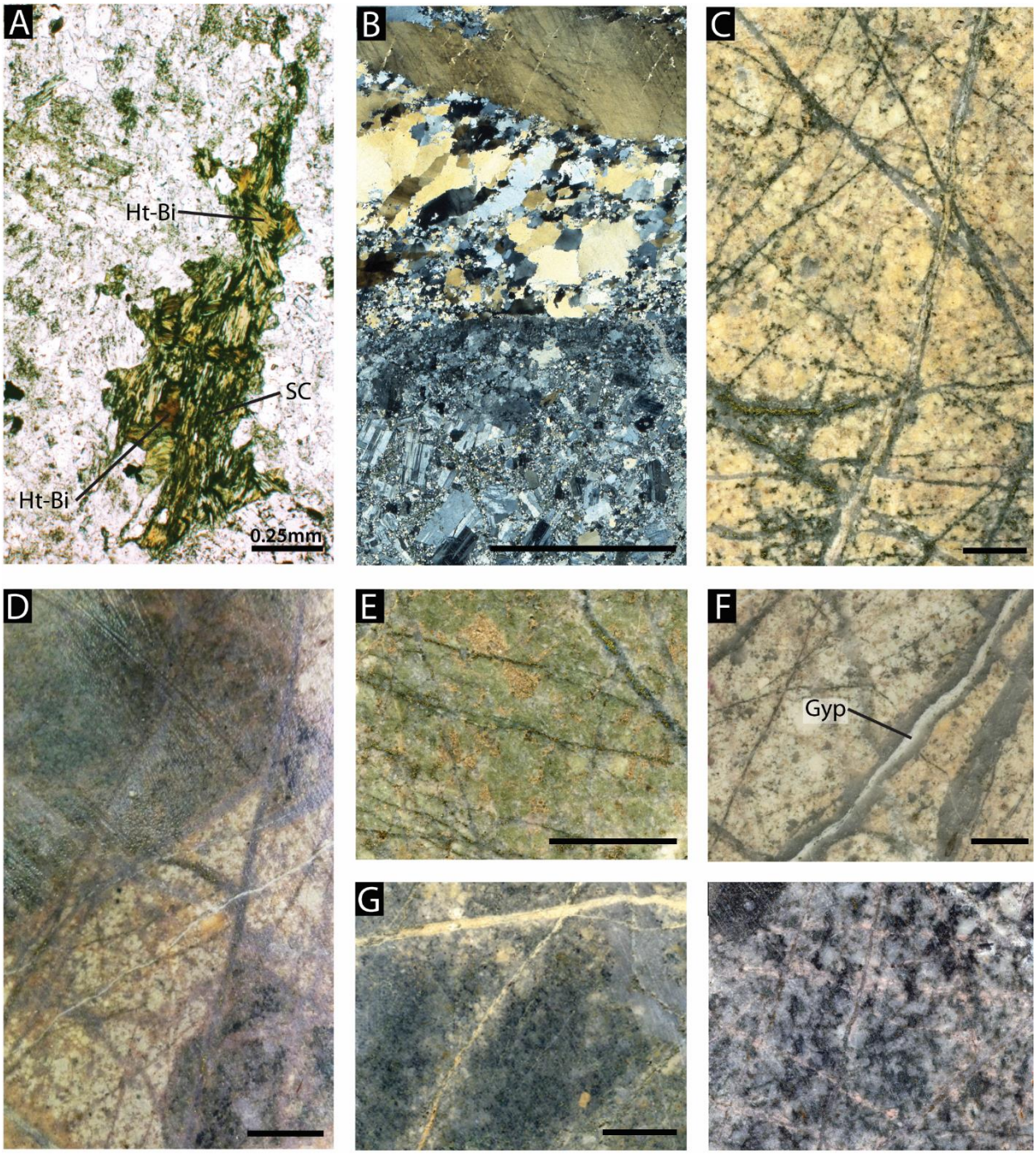

Figure 7: Photographs of veins and age relationships between veins, scale is 1 cm for all photos unless otherwise noted. A. Photomicrograph example of hydrothermal biotite alteration of hornblende partially converted to shreddy chlorite (SC). B. Barren A quartz vein with quartz crystals recrystallized under strain along wall rock contact. C. Stockwork quartz veins with pervasive tan sericite + quartz alteration of the wall rock. D. Pervasive tan and pale green sericite alteration of wall rock bounded by older stockwork quartz veins. Alteration is notably asymmetric around quartz veins indicating wall rock alteration occurred post-formation of the quartz veins. E. Pervasive pale green sericite alteration with quartz veins and chalcopyrite veinlets. F. Gypsum reopening and infilling quartz vein. G. Tan sericite infill on vein/fracture. H. K-feldspar selvage developed on fractures that are crosscut by quartz veins.

fluids was noted by Gustafson and Hunt (1975) at the El Salvador deposit. It is likely that at depths greater than current drilling anhydrite is more abundant than gypsum as was observed at depth at El Salvador.

Sulfide Mineralization and Zoning:

Ore at Botija is hosted entirely within hypogene sulfides with only minor copper oxides present in saprolite exposures. The saprolite blanket ranges in thickness from 5 – 50 m but generally is between 25 – 50 m. There is no significant Cu oxide enrichment in the saprolite. Pyrite and chalcopyrite are the dominate sulfide species in Botija, but bornite locally occurs in chalcopyrite rich zones. The majority of pyrite is primarily associated with late phyllic alteration and occurs in both D veins and as disseminated replacement of hornblende crystals. Copper is dominantly hosted within chalcopyrite at Botija, occurring mostly as a disseminated replacement of hornblende sites spatially associated with quartz veins and K-Silicate alteration. Minor bornite associated with chalcopyrite is observed at depth at Botija in several drill cores, including within AB and B veins and locally disseminated into the wall rock, but does not contribute significantly to the overall copper endowment of the deposit. Molybdenum is hosted in molybdenite, and is hosted in B and quartz-molybdenite veins. Whereas vein-hosted copper iron sulfides are present in Botija, they are volumetrically minor compared to disseminated chalcopyrite. Chalcopyrite to pyrite ratios greater than 1:2 are associated with high grade copper (>0.5 wt.%). Generally, the pyrite-dominated domains overlie the chalcopyrite- (and copper-) rich intervals of drill core. Sulfide distribution for holes which were not logged was classified from whole rock geochemistry using a ternary plot of Cu, Fe, and S (Figure 8). In the core of the deposit, copper grades >0.3 wt.% are associated with intervals classified to be dominantly chalcopyrite to a mixture of chalcopyrite

and pyrite and this zone is enclosed in a pyrite-rich zone with low grades of copper (<0.5 wt.%). The spatial distribution of sulfides in the deposit will be further explored below.

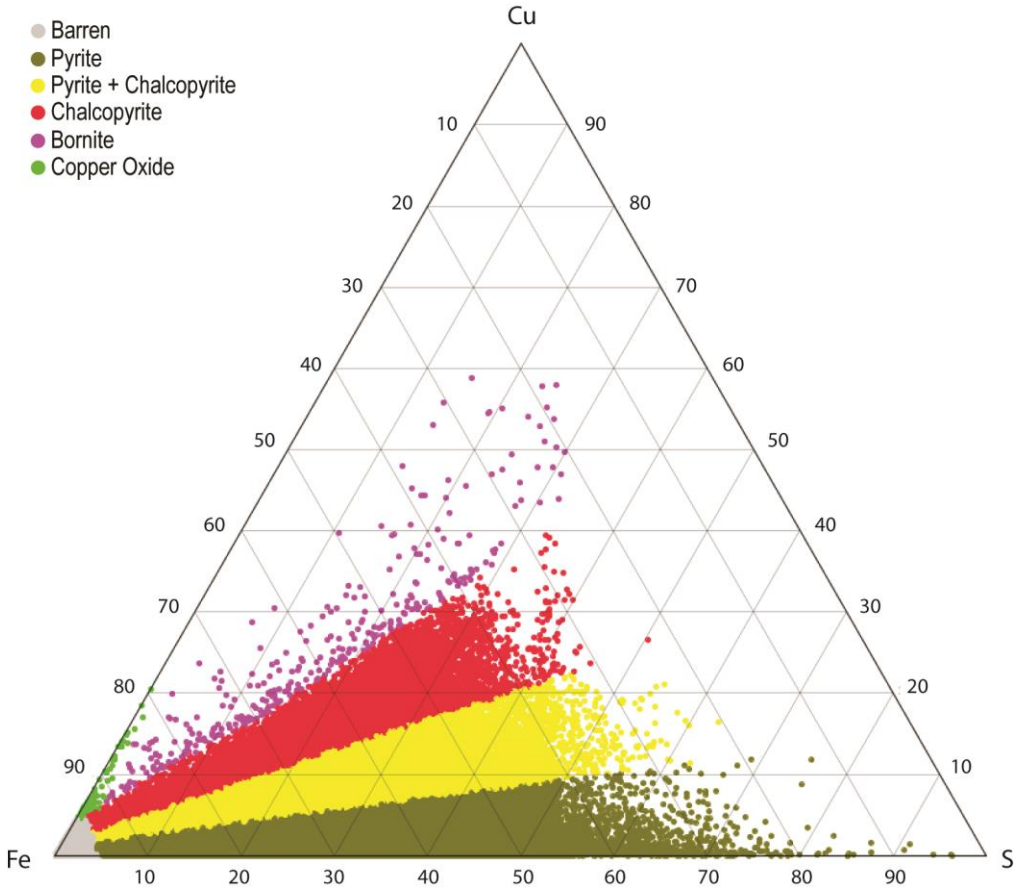

Figure 8: Ternary Cu-Fe-S diagram of diamond drill core samples (wt.%) from Cobre Panamá. Sulfide composition for each sample has been classified based on ratio of copper and iron to sulfur.

STRUCTURE

Vein Orientation:

Vein orientation measurements on early quartz (n = 464) and hydrolytic (n = 1027) veins were collected from five oriented drill holes and nine trench mapping localities. Early quartz veins include A, AB, B, and quartz-molybdenite veins whereas hydrolytic veins include D and pyrite veinlet veins. These measurements were integrated with measurements from the existing FQM dataset and previous studies (Speidel and Faure, 1996; Nobel and Benavides, 2013; 2014) (Figure

9). D veins generally show strike orientations with range 0-360° but have dominant mode at strike/dip of 295/73°NE, 260/69°NW, and 228/48°NW. In comparison quartz vein orientations are more restricted; quartz veins have strikes ranging from 185 - 320° with dominate strike/dip orientations of 292/45°NE and 233/50°NW. Early quartz veins also have two subordinate gently-dipping sets which are oriented 004/22°E and 201/26°W. Vein dips were also recorded from logged vertical unoriented drill holes, these dips show agreement with the bimodal shallow and moderate to steeply dipping early quartz and D veins measured from drill core and trench mapping.

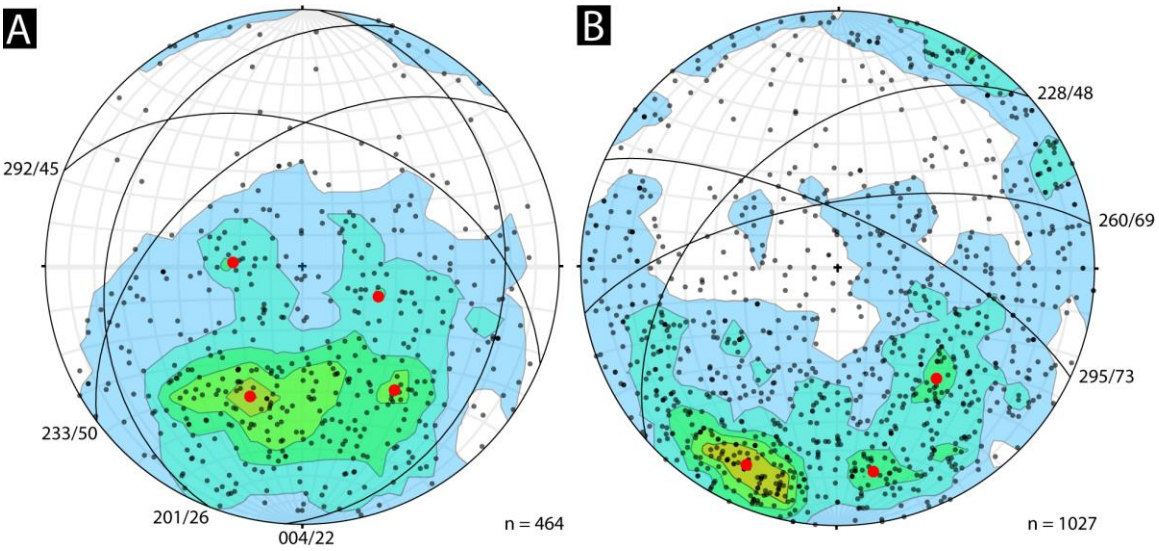

Figure 9: Equal-area, lower-hemisphere stereonets projections of poles to planes for veins, poles are colored in a color scale based on density of poles (light grey to black based on increasing pole density). Poles are Kamb contoured using a contour interval of 2σ and a counting area of 1.9% of net area, average poles (red dots) are plotted for the dominate vein orientations. Average planes (great circles) of veins are plotted on stereonets as well. A. Steronet of poles to all quartz veins (A, AB, Qz-Mb) showing modes at 292/45°NE, 233/50°NW, 004/22°E, and 201/26°W (n=464). B. Steronet of D veins with pole modes of 295/73°NE, 260/69°NW, and 228/48°NW (n=1027).

D veins were mapped in available saprolite roadcut exposures across the deposit and allow for spatial variation in vein orientation to be discerned (examples of field trench maps are presented in Figure 10). Over the center of the orebody, D veins formed a stockwork of all three

orientations noted in Figure 9, whereas, outboard of the orebody, D veins occur along preferential orientations. To the west of the deposit, D veins formed in sheeted sets with two strike orientations generally at 45° angles to each other with modal preferred orientations of strike/dip of 290/75°NE and 155/80°SW or 335/70°NE (see West Botija - Figure 10). North and south of the deposit, the D veins have modal preferred orientation with strike/dip of 190/60°W and 005/80°E. No mapping exposures were available to the east of the orebody to document if this trend in vein orientation is symmetrical around the orebody.

The moderate to shallow dip of the veins at Botija, particularly the quartz veins, is atypical for a porphyry copper deposit. Most early high-temperature veins are emplaced subvertically in orthogonal set along tensional hydrofractures with a subordinate group which are flat dipping (<20°) (Tosdal and Richards, 2001). These observations have been documented in numerous porphyry deposits globally including Bingham Canyon (Redmond and Einaudi, 2010), Butte (Houston and Dilles, 2013), San Juan (Heidrick and Titley, 1982), Henderson (Carten et al., 1988), and Sierrita-Experanza (Titley et al., 1986). Late D veins have also been identified to commonly dip steeply at El Salvador (Gustafson and Hunt, 1975) and Bajo de la Alumbrera (Proffett, 2003), however, the orientation of D veins at Butte have also been documented to have been influenced by tectonic stress and exhibit a much larger range of dips (Proffett, 1973; Houston and Dilles, 2013). Rock mechanical theory and numerical modelling of upward moving fluid plumes from crustal magma chambers support these observations and demonstrate that hydrofracturing is the emplacement mechanism for early high temperature veins in porphyry systems whereas lithostatic stresses influence late veins as the system cools (Tosdal and Richards, 2001; Weis et al., 2012).

The strike of early veins in porphyry deposits is less understood in comparison to their dip. Some deposits, notably Henderson (Carten et al., 1998), have steeply dipping radial and lesser shallow concentric high-temperature veins which form concentrically around a central porphyry stock whereas most deposits such as Bingham Canyon (Redmond and Einaudi, 2010), Butte (Houston and Dilles, 2013), Sierrita-Esperanza (Titley et al., 1986), and Copper Mountain (Stanley et al., 1995) have orthogonal sets of high-temperature veins where one orientation of veins tends to dominate.

The veins at Botija share many similarities with examples from other porphyry deposits, because early high temperature quartz veins (Figure 9a) have two dominant orientations, (292/45°NE and 233/50°NW) with a preferred orientation of 292/45°NE. These veins differ from other deposits noted above in their moderate dip (45-50°). The moderate dip of quartz veins is interpreted to suggest approximately 40° of southward tilting from originally vertical orientation. D veins have a much wider range of strike orientations compared to quartz veins (Figure 9b) and mostly range in dip from moderately to steeply dipping (48-73°). Poles to planes of D vein orientation measurements form a girdle, which indicates a concentric habit to D veins, however, D veins do have preferred orientation of 295/73°NE, which is similar in strike orientation but with slightly steeper dips than quartz veins. A tilt restoration of 40° to the northwest about a 060/240° northeast-southwest axis restores both the early quartz and D veins to vertical.

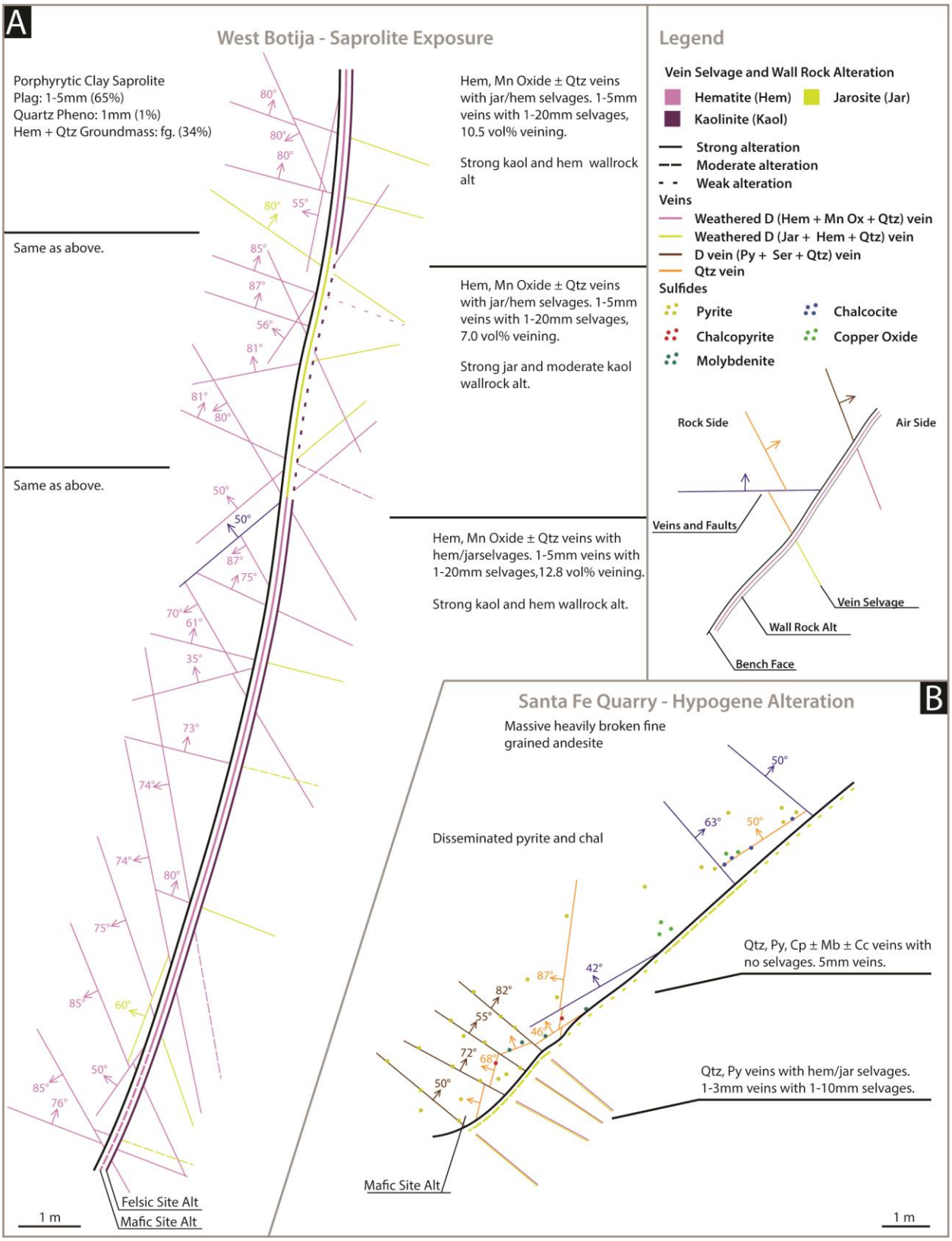

Figure 10: Example of geologic bench mapping conducted in Botija using Anaconda method (Einaudi, 1997). A. Stockwork weathered D veins in saprolite. B. Hypogene alteration and mineralization with quartz veins cut and offset by D veins.

Post-Ore Faults:

The presence of post-ore fault offsets at the Botija deposit has been recognized by geologists as early as the mid-1970s. Several generations of geologists have identified the east-west striking and north-dipping Botija fault in addition to more cryptic NE and SW striking faults in the western half of the deposit (Speidel and Faure, 1996). Despite four decades of geological investigation at Botija, poor field exposure has restricted the ability to constrain the location or kinematics of faults. Observation of kinematic indicators from drill core and outcrop provide evidence for interpretation of normal, thrust, and strike-slip sense of movement, sometimes on the faults with the same orientation (Nobel and Benavides 2013; 2014; Speidel et al., 2001).

Since the majority of drill cores logged were not oriented and core orientation was often not possible through large fault zones due to poor rock competency (i.e. gouge zones) measurement of fault orientation and kinematic indicators was often not possible. Due to these issues, it was not possible to construct a large dataset of fault orientation as was done with quartz and D veins, with the unquantifiable uncertainty in individual measurements from drill core orientation there are not sufficient data to fully understand the structural geologic history. Instead, this study has focused on the identification of the location of faults from drill core and integrated these observations with available geotechnical data from unlogged holes, and surface mapping from previous studies (Speidel and Faure, 1996; Nobel and Benavides 2013; 2014) to constrain the orientation of major faults. Fault kinematics were inferred from the restoration of the magmatic-hydrothermal alteration system associated with the emplacement of the orebody. The vein paragenesis defined at Botija (Figure 5) indicates that an evolution of magmatic-hydrothermal system follows a simple temporal progression from high to low temperature alteration and

mineralization. This simple evolution of veins suggests a classical alteration zonation as defined by numerous previous studies (Lowell and Gilbert, 1970; Gustafson and Hunt, 1975; Dilles, 1987; Dilles and Einaudi, 1992; Proffett, 2003) is an appropriate model for the Botija deposit, and therefore, juxtapositions of different vein types and alteration assemblages can be used to constrain kinematics on faults.

Faults observed in drill core cut all magmatic-hydrothermal veins associated with the formation of the porphyry copper deposit (Figure 11c). The majority of faults are brittle in nature with some of the larger faults having evidence for brittle and ductile deformation of mica- and clay-rich incompetent rocks (Figure 11e). Major faults are typically 10s of centimeters in apparent thickness with only a few of the larger faults extending to 1 – 5 meters in thickness. Faults are commonly characterized by clay gouge zones (Figure 11a), cataclasite (Figure 11d), and occasionally shear fabrics. Numerous small centimeter-scale (1 – 10 cm width) faults are present throughout the deposit but commonly are most abundant for 10s of meters into the hanging wall of major faults. Small faults are commonly filled with zeolite and to a lesser degree chlorite and clay (Figure 11b). Intensity of zeolite alteration generally increases towards large faults and commonly destroys original rock texture in the core of a fault zone. Zeolite alteration continues into the hanging wall of major faults along small centimeter-scale faulting to produce a light pink color to wallrock. Thin sections of these zones show zeolite as a fill mineral to open space fractures or as the matrix material in fault cataclasites (Ross and Thompson, 1996). As noted above, zeolite alteration entirely post-dates Cu-Fe sulfides, providing additional evidence that faults post-date all ore formation.

Three cross-sections have been constructed from the collected drill core data and their locations are presented on a plan map of the deposit (Figure 12). Faults locations, quartz and D vein volume percent, copper concentration, and Cp:Py ratios are compiled for the three sections. An East-west cross-section 977200N (A-A') is presented in Figure 13, north-south cross-sections 538100E (B-B') and 538900E (C-C') are presented in Figure 14 and Figure 15, respectively.

Botija and Santa Fe Fault Zones: Two east-west striking fault systems are present at the Botija deposit, the Botija and Santa Fe fault zones. The Botija and Santa Fe fault zones have strike/dip of 275/50°N and 268/70°N, respectively. The Botija Fault was one of the earliest identified structures, and it locally bounds or offsets copper grade at the southern extent of the orebody (see B-B' Figure 14). The Botija River has been noted to run along the Botija fault in previous mapping studies (Speidel and Faure, 1996; Nobel and Benavides 2013) The northern extent of the orebody is bounded by the Santa Fe fault (see B-B' Figure 14). The distribution of aplite dikes varies across the Botija and Strike Central faults. Whereas only rare aplite dikes are observed in the hanging wall of the Botija fault in section C-C' (Figure 15), swarms of aplites dikes up to 2.8 vol.% were encountered in the foot wall of the Botija fault in drill hole B14046. To the north of the Santa Fe fault aplites swarms up to 1.0 vol.% are present at shallow levels (0-450 m depth) in drill core at shallow levels in drill hole B12163-HG (see Figure 12 for location). Additionally, B12163-HG was the only drill hole logged where the majority of the hole (>85%) was in equigranular Petaquilla granodiorite, further supporting the notion that a deep level of the magmatic-hydrothermal system is present in the hanging wall of the Santa Fe fault. The presence of the highest vol.% of aplites in the hanging wall of the Santa Fe and foot wall of the Botija faults

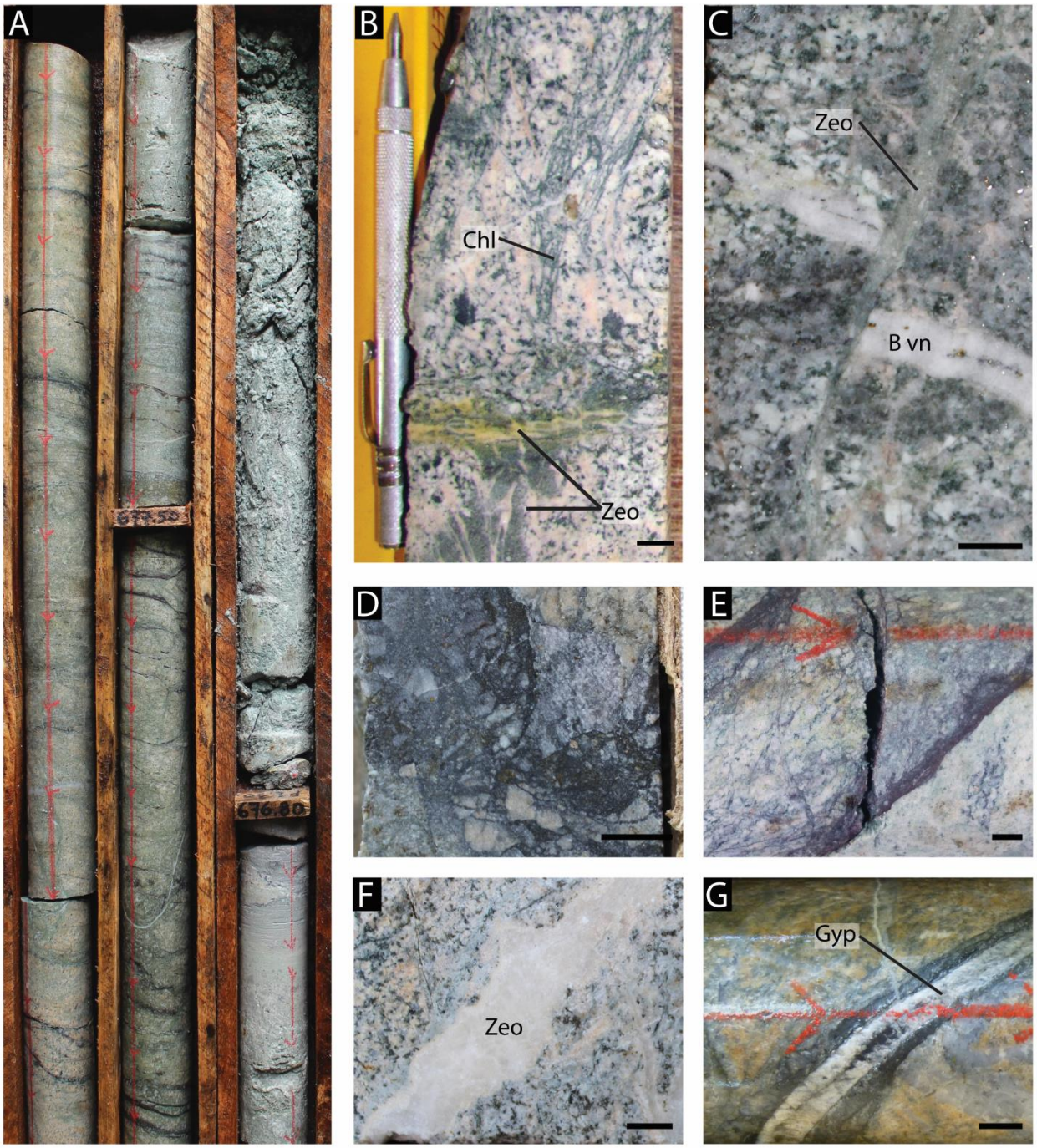

Figure 11: Photographs of structural textures, scale is 1 cm for all photos. A. Downhole intersection of the 33 m wide Botija Fault Zone in drill hole B15002. Fault zone is characterized by 0.5 m scale clay gouge zones (B15002 676.0 – 676.8 m; Figure 14) bounded by brittle faults filled by zeolite (B15002 676.8 – 678.8 m; Figure 14). B. Horizontal zeolite filled fault with orthogonal chlorite and zeolite fracture fill emanating from fault. C. Zeolite filled fault offsetting B quartz vein. D. Fault cataclasite with zeolite alteration of clasts. E. Brittle-ductile fault zone with sheared and zeolite altered wall rock clasts with clay gouge zones forming along planar wall rock contacts of the fault zone. F. Zeolite filled vein cutting porphyritic granodiorite. G. Gypsum filling center of gouge filled fault.

suggests the mineralized interval between these faults has been down-dropped by at least 400m based on depth of logged drilling. This suggests normal movement on the Botija fault and reverse movement on the Santa Fe fault. Copper mineralization and K-silicate alteration is present in the hanging wall of the Botija Fault in the west end of the deposit, whereas altered and mineralized rock is present in the footwall to the east indicating left lateral oblique normal slip on the Botija fault has down dropped copper ores and k-silicate alteration to the northwest. Oblique motion is difficult to constrain from drill core, however, the limited measurements available do provide indication that normal dip slip movement has occurred on the Botija Fault. Movement on the Santa Fe fault is difficult to resolve due to the lack of logging to the north of the deposit; the kinematics on the Santa Fe fault will be discussed later.

Northwest Striking Faults: A NW striking corridor of faults is present throughout the Botija deposit. These faults strike between 312 - 322° (NW) and dip steeply, approximately 75°NE. Limited fault orientations measured from drill core indicate the two steeply dipping and northwest striking fault zone that strikes 292-320° and dips 60-90°NE exists in the deposit. Two of these faults are described below as Oeste and Este faults These faults are not well exposed and have not been identified in surface exposures in this or previous studies, hindering understanding of their extent or orientation, however, stream drainage channels are observed to follow the fault traces that are projected from drill core intersections. The Oeste fault cuts and bounds quartz veining and copper mineralization along the western end of the deposit (see A-A' Figure 13). The foot wall of this fault notably contains no significant quartz veining or copper mineralization but has been hydrothermally altered to a K-silicate assemblage, with mafic sites replaced by shreddy chlorite after hydrothermal biotite. The sharp break from strongly

mineralized and quartz-veined hanging wall to a barren foot wall requires in excess of 250 m of normal or dip slip displacement based on the depth of logged drilling, juxtaposing a mineralized hanging wall against a deep barren K-silicate altered footwall rock. While the Este fault can be identified to follow a similar orientation to the Oeste fault, a lack of drill data east of the deposit prevents better constraint the orientation of the fault.

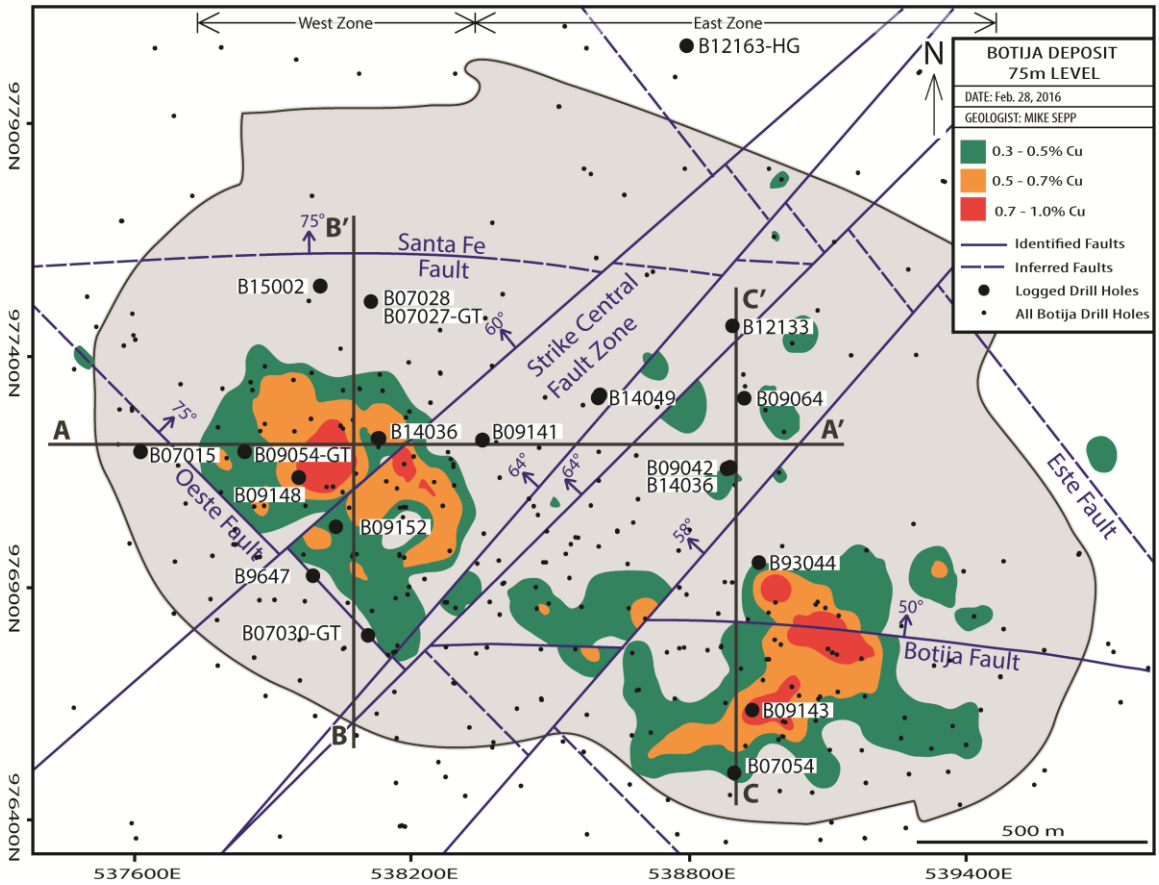

Figure 12: Plan map of the Botija deposit at 75 m elevation (about 50 m below surface) with copper grades contoured and interpreted locations of major faults plotted in blue, the extent of the termed west and east zones of the deposit are labelled. Collars of drill holes logged along three cross-sections are plotted on the map. An additional 518 holes were used to construct Cu grade contours. Three cross-sections are constructed from these drill holes, one east west on the 977200 northing (A-A') and two north-south on the 538100 and 538900 easting
(B-B' and C-C' respectively).

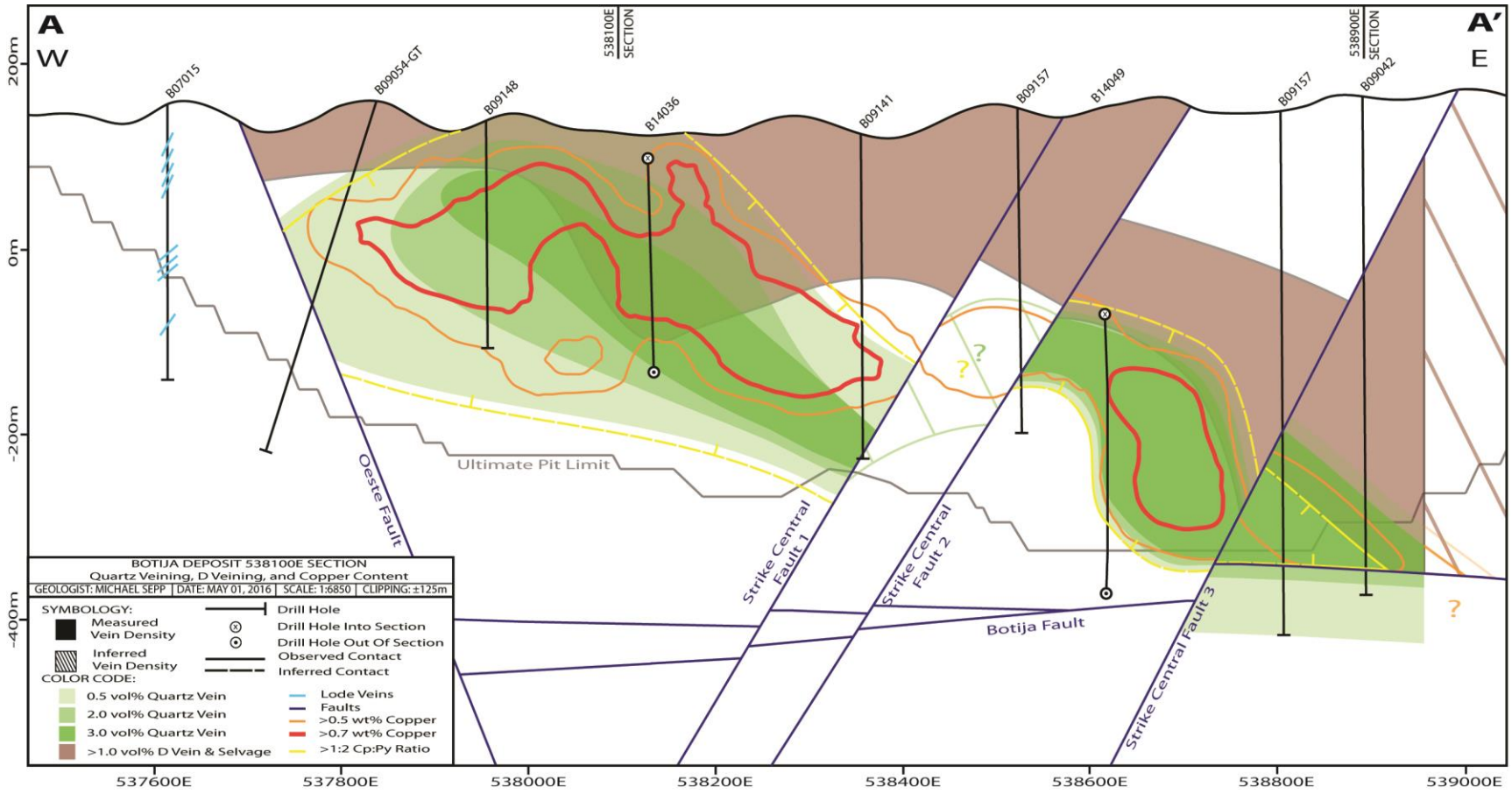

Figure 13: North-south cross-section A-A' (looking north) constructed on the 977200 northing, clipping on the section is ±125m. Quartz veins densities of 0.5, 2.0, and 3.0 vol% are contoured in orange whereas D vein densities >1.0 vol% are shown in brown. Ratios of chalcopyrite to pyrite >1:2 from logging are plotted in red. Copper contours of 0.5 and 0.7 wt% from 3D modeling utilizing the entire drilling dataset are contoured in purple. The location and dip angle of lode veins is shown in green.

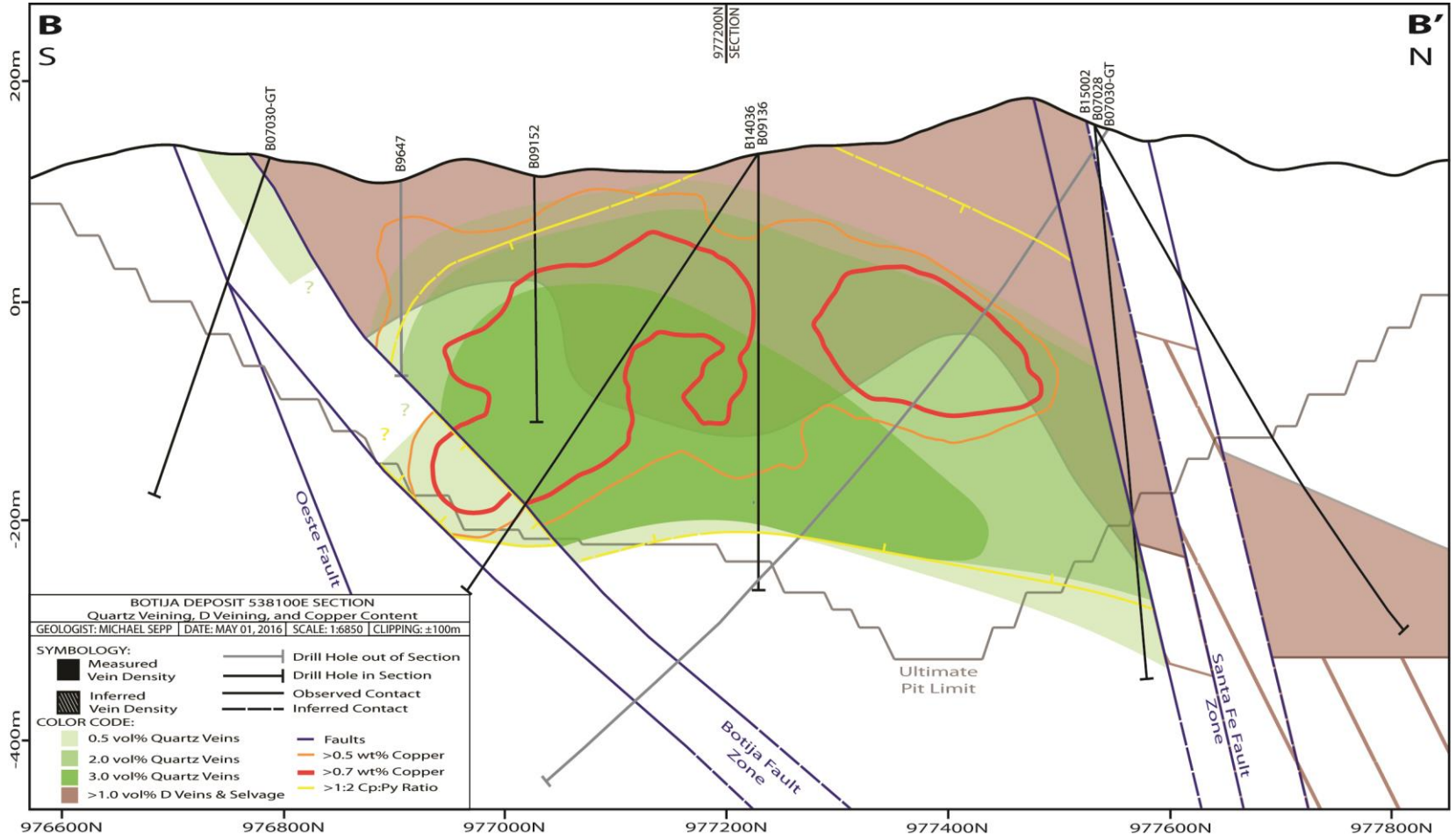

Figure 14: West-east cross-section B-B′ (looking west) constructed on the 538100 easting, clipping on the section is ±100m. Quartz veins densities of 0.5, 2.0, and 3.0 vol% are contoured in orange whereas D vein densities >1.0 vol% are shown in brown. Ratios of chalcopyrite to pyrite >1:2 from logging are plotted in red. Copper contours of 0.5 and 0.7 wt% from 3D modeling utilizing the entire drilling dataset are contoured in purple.

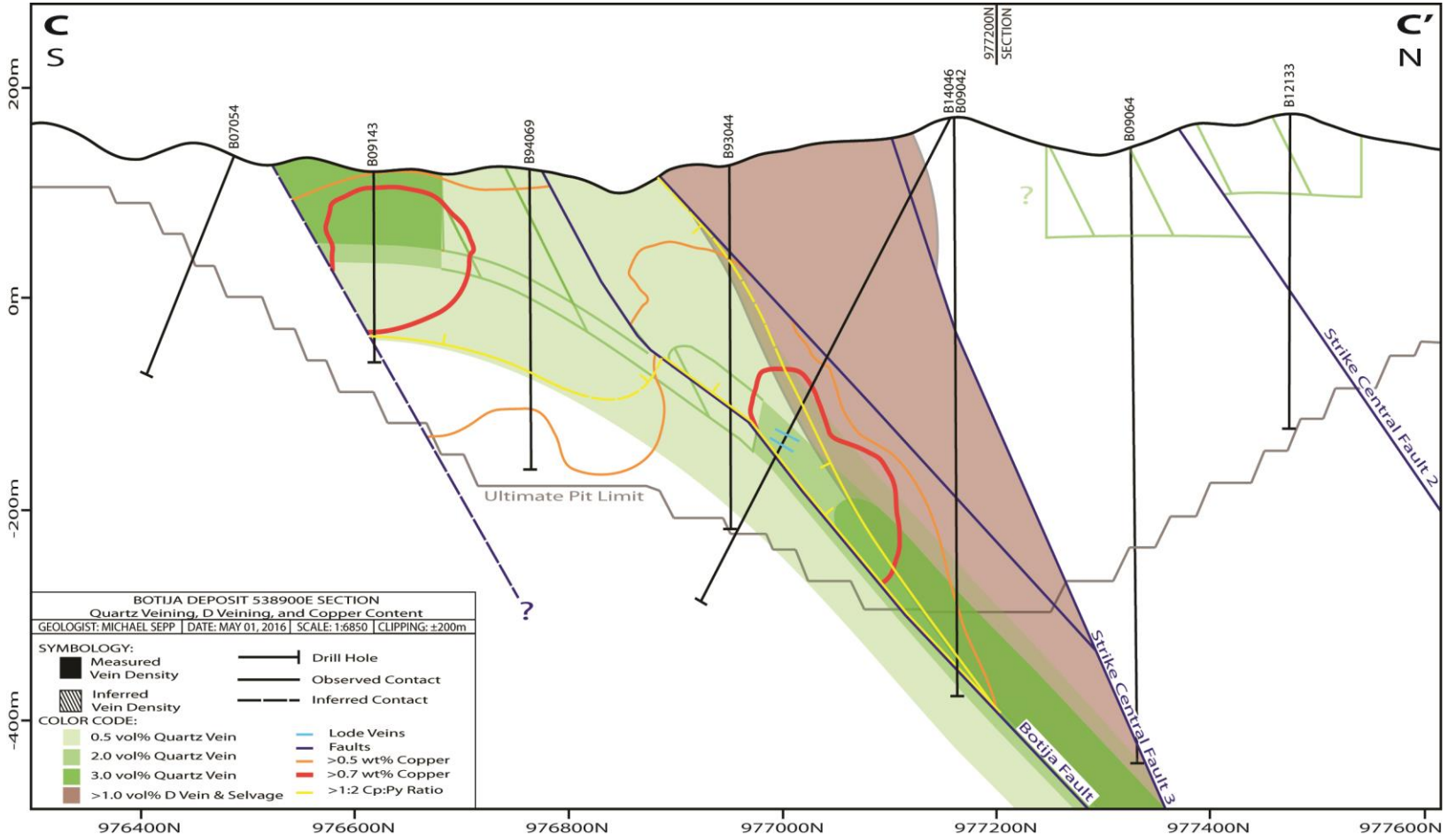

Figure 15: West-east cross-section A-A' (looking west) constructed on the 538900 easting, clipping on the section is ±200m. Quartz veins densities of 0.5, 2.0, and 3.0 vol% are contoured in orange whereas D vein densities >1.0 vol% are shown in brown. Ratios of chalcopyrite to pyrite >1:2 from logging are plotted in red. Copper contours of 0.5 and 0.7 wt% from 3D modeling utilizing the entire drilling densities are are are contoured in purple. The location and dip of lode veins is shown in green.

Strike Central Fault Zone: The Strike Central fault zone consists of a series of faults which strike 200-225° (SW) and dip 60-65°NW through the center of the deposit. The fault zone is 550-650 m in width and includes four major fault strands based on geologic interpretation of drill core, however, numerous smaller faults are present in the fault zone. Drill core observations supports field mapping by Speidel and Faure (1996), and identified numerous faults in stream outcrops over the core of the deposit which strike between 200 - 260° and dip an average of 65°NW. Breaks in hydrothermal alteration, mineralization, and zones of exceptionally poor rock quality identified in geotechnical data correlated with faults identified from surface mapping. Cross section A-A' (Figure 13) shows the displacement of the hydrothermal system by these faults. Offsets in the quartz and D veins, Cp:Py ratios, and copper mineralization show 10s-100s of meters of displacement with a minimum estimate for the fault zone of 350m. The truncation of D veins across Strike Central fault provides a minimum fault offset in excess of 500 m (see C-C' Figure 15).

These offset estimates are apparent due to the oblique angle of intersection of the cross sections with the fault zone. The displacements identified in these cross sections require normal or dip slip displacement on the Strike Central fault zone as thrust or strike-slip displacement would not explain the current northwest elongation of the deposit. The limited amount of fault orientation measurements available from drill core support the interpretation of faults offsetting hydrothermal alteration and mineralization with this orientation, however, an additional set of southwest striking faults which dip much shallower, 35°W-NW, are also present. Field mapping by previous studies (Speidel and Faure, 1996; Nobel and Benavides, 2013; 2014) have demonstrated the Strike Central fault zone cuts the older Botija, Santa Fe, and NW fault zones in field exposures. The orientation of rivers which follow the Botija, and NW faults are noted to

change to southwest-northeast when the Strike Central fault zone is intersected, providing additional field evidence that the Strike Central fault system is the latest generation of faulting.

CHANGES IN VEINS, ALTERATION, AND MINERALIZATION ACROSS FAULTS

Hydrothermal Alteration and Mineralization:

Quartz vein density in the deposit ranges from 0 – 20 vol.% but generally does not exceed 3 vol.%. Locally quartz vein densities >7 vol.% are observed (i.e. B14049 344 – 419 m downhole Figure 13 and B14036 180-300 m downhole Figure 14) but these intervals are not correlatable between drill holes. Spatially, quartz vein density abruptly changes across the east-west oriented Botija and Santa Fe faults, the Oeste fault, and the Strike Central fault zone. Whereas it has been documented that quartz vein density increases towards the core of the magmatic-hydrothermal system beneath the copper ore body at Bingham Canyon (Gruen et al., 2010; Redmond and Einaudi, 2010), El Salvador (Gustafson and Quiroga, 1995), and Butte (Rusk et al., 2008), no such relationship is present at Botija. In section B-B' quartz vein density generally increases with depth, however, in cross-section A-A' and C-C' no distinct spatial zonation can be discerned. Barren quartz veins with well-developed potassic alteration selvages are present (2.5-18.6 vol.%) only at depth in section C-C' in the foot wall of the Botija fault but are scarce (>1.0 vol.%) in at depth in section B-B'. These veins are documented at other deposits to predominantly occur in the high temperature zones (Sillitoe, 2010), representing a deeper part of the porphyry copper magmatic-hydrothermal system. The lack of A type quartz veins at depth in the three cross-sections logged suggests that fault displacement separates the deep barren vein zones from the overlying well-mineralized ore zones.

D veins are also cut by the brittle faults, of the Botija and Santa Fe fault zones (Figure 14), the Oeste fault (Figure 13), and Strike Central fault zones (Figure 13 & Figure 15) causing sharp truncations in the extent of >1 vol. D veins + selvages. Though the density of D veins (vol.%) is often highly variable on a scale of 10s of meters, the extents (>1 vol.% D veins + selvages) of D veins and their selvages is usually continuous for over 1000 m of meters upward and outboard from the high temperature core of these systems. Nonetheless, it is common for D veins to also extend deep into older K-silicate altered zones (Sales and Meyer, 1948; Lowell and Guilbert, 1970; Gustafson and Hunt; 1975; Dilles and Einaudi, 1992).

Copper grades >0.5 wt.% are associated with intervals with quartz veins >0.5 vol.%, however, there is no simple and direct correlation between higher quartz vein density and copper grades. Chalcopyrite to pyrite ratios >1:2 are spatially associated with quartz veins and copper mineralization and are also truncated by the Botija (Figure 14; Figure 15) Santa Fe zones (Figure 14), Strike Central (Figure 13, Figure 15), and Oeste fault zones (Figure 13). Modeled high grade (>0.5 wt.%) copper ore shells, similar to quartz veins, are clearly cut and offset by post-ore faults. In section 538100E (Figure 14) high grade copper is continuous and forms a broad flat-lying convex-shaped up body (Figure 14) measuring approximately 700 m (length) x 400 m (width) x 200-375 m (height). To the east across the Strike Central fault zone the ore body is highly dismembered in tabular to curved annulus pieces near Strike Central faults 2 and 3 (Figure 13) whereas tabular segments occur in the hanging wall of Botija fault zone Figure 15). These dismembered tabular to cylindrical pieces resemble the limbs and the broad convex shaped ores of the west zone of the deposit resembles the top, respectively, of a classic inverted tea cup shaped geometry typical of a porphyry copper deposit.

Molybdenum concentrations >50 ppm generally sit at the edge and immediately outside the central zones of high grade copper (>0.5 wt.%) and have the same irregular geometry as copper, with a more clearly definable inverted tea cup shaped shell geometry in the west zone. Despite low gold concentrations in Botija, gold grades >0.1 g/t can be correlated between drill holes and fault offsets are less apparent. Gold spatially coincides with high grade copper but is preferentially concentrated in the west zone of the deposit.

Fault Kinematics:

The fault kinematics can be constrained by the breaks in hydrothermal alteration, copper mineralization, and changes in copper grade across faults (Figure 16). High density of quartz and D veins and high copper concentrations are localized in the hanging wall of the Botija Fault on the western or B-B' section (Figure 14). High quartz vein density and copper grades are observed within the Botija Fault zone, however, the alteration and copper mineralization is discontinuous. In the foot wall of the Botija fault on section B-B' (Figure 14) there are no significant quartz veins or copper mineralization present. K-silicate alteration and associated quartz veins are also truncated by the Botija fault, with the foot wall containing only sparse quartz veins (<0.5 vol.%) with K-silicate alteration. On the eastern or C-C' section (Figure 15) quartz vein density and copper grades occurs in a tabular north-dipping geometry in the hanging wall of the Botija fault and as an approximately flat lying body in the foot wall of the Botija fault at higher elevation. Below 100 m elevation (sea level datum) in the footwall of the Botija fault, quartz vein density is low (~0.5 vol.%) in comparison to the hanging wall (1-3 vol.%) but is more erratic with intervals locally ranging up to 18.6 vol.%. Copper grade >0.2 wt.% is also constrained to the hanging wall of the Botija fault below 100m. Vein type also varies across the Botija fault at depth where

mineralized AB quartz veins are present in the hanging wall of the fault whereas barren quartz veins with well-developed K-feldspar selvages are present in the foot wall. Barren quartz veins are characteristic of the deep core of the magmatic-hydrothermal system (Seedorff et al., 2005). The presence of aplite dike swarms in the foot wall below the Botija fault in section B-B' further supports the interpretation of the foot wall being a deep level of a porphyry copper system. The transition between mineralized to barren quartz veins is usually a transition which occurs over 100s of meters in most porphyry copper deposits. The sharp juxtaposition of mineralized and barren quartz veins across the Botija fault provides compelling evidence of normal displacement. These observations of the high temperature hydrothermal alteration and copper mineralization provide a minimum estimate of 500m left lateral oblique normal displacement can be made for the Botija fault.

Copper mineralization and quartz veins are abruptly truncated by the northwest striking Oeste fault, Copper grades are generally <0.15 wt.% and quartz vein density <0.5 vol.% in the foot wall of the Oeste fault (Figure 13) compared to Copper grades of locally >0.7 wt.% and quartz vein density >1.0 vol.% in the hanging wall in sections A-A' and B-B' (Figure 13; Figure 14). The presence of K-silicate alteration and lack of quartz veining in the foot wall suggest a deep level in the hydrothermal system indicating normal displacement on the Oeste fault. Nonetheless, as previously mentioned, a component of oblique slip cannot be ruled out (at this point) due to a paucity of map and dill core data southwest of the Oeste fault at the Botija deposit.

The geometry of hydrothermal alteration and ore shells at Botija is dramatically different between the three cross-sections. The 0.5 wt% copper ore shell in western cross-section B-B' (Figure 14) is a flat lying convex shaped body with lateral continuity of approximately

400 – 700 m in both width and length dimensions. The 0.5 wt.% ore shell in eastern cross-section C-C' has a markedly different geometry (Figure 15). a tabular ore shell approximately 50-100 m in thickness and dips 50° N in the hanging wall and 10°N in the foot wall of the Botija fault. East-west cross-section A-A' (Figure 13) links the two north-south cross-sections and illustrates the east-west irregularity of the orebody. Integrating observations from the three cross-sections together, the Botija ore body appears to be characterized by two different zones, a west zone in the hanging wall of the Strike Central fault zone and an east zone within the splays and into the foot wall of the Strike Central fault zone. Across the four identified strands of Strike Central faults, the ore body of >0.5% Cu is stepped as a series of fault bounded, irregular tabular to annulus bodies that dip moderately to the northeast and have restricted widths on the scale of 10-50m meters compared to the flat lying planar ore body in the hanging wall of the Strike Central fault zone. AB quartz veins in the west zone are generally more abundant with a density range of 1-11 vol.% compared to the footwall of the Strike Central fault zone with density range of 0.5-7.5 vol.%. Copper grades >0.7 wt.% mostly occur in the west zone, whereas in the footwall of the Strike Central fault zone copper grades are dominantly between 0.4-0.6 wt.%. The change in geometry of the ore shells and quartz vein type suggests that normal displacement has occurred on the Botija and Strike Central faults and moved the top of the copper mineralization shell down and to

the northwest.

Whereas strike-slip faulting is the dominate form of deformation on the isthmus of Panamá, the majority of the faults at Botija do not exhibit the common characteristics of strike-slip faults. The faults of Botija generally dip moderately (50-75°) and have damage zones on the

order of 10s meters that are commonly infilled by zeolite. Common strike-slip faults tend to dip steeply (generally >70°) and tend to have wide damage zones that are symmetrical around the main fault trace, whereas at Botija deformation is primarily observed in the hanging wall of faults. Additionally, the <75° dip of many of the faults would prove difficult to have initiated from strike-slip motion. A study by Segall and Pollard (1983) of strike-slip faults in similar composition rocks of the central Sierra Nevada, California, concluded that strike-slip faults developed in granodiorite with dips in excess of 70°. With the exception of the Oeste and Santa Fe faults, which dip 75°NE, the dips (<70°) of the Botija, and Strike Central Fault zones is indicative of normal or oblique normal movement.

Cryptic Low Angle Faults:

Whereas current field exposures and drill cores inhibit the recognition of faults outside of the immediate deposits areas, ZTEM™ (z-axis tipper electromagnetic) geophysical data provides insight into covered structure in the Cobre Panamá mining camp. ZTEM™ is an airborne audio-frequency magnetics system which uses passive electromagnetic fields to measure lateral resistivity contrast in the earth (Legault, 2010). Vertical variation in resistivity can be calculated from lateral resistivity collected in the survey using a linear relationship defined by Vozoff (1972). ZTEM™ surveys are able to measure changes in resistivity up to 2 km in depth (Legault, 2010). Changes in resistance can be used to interpret geologic features at depth below surficial cover, however, ZTEM™ surveys measure bulk rock resistivity which is an integrated value from the sum of geologic processes which have occurred and therefore care must be taken no to over interpret data.

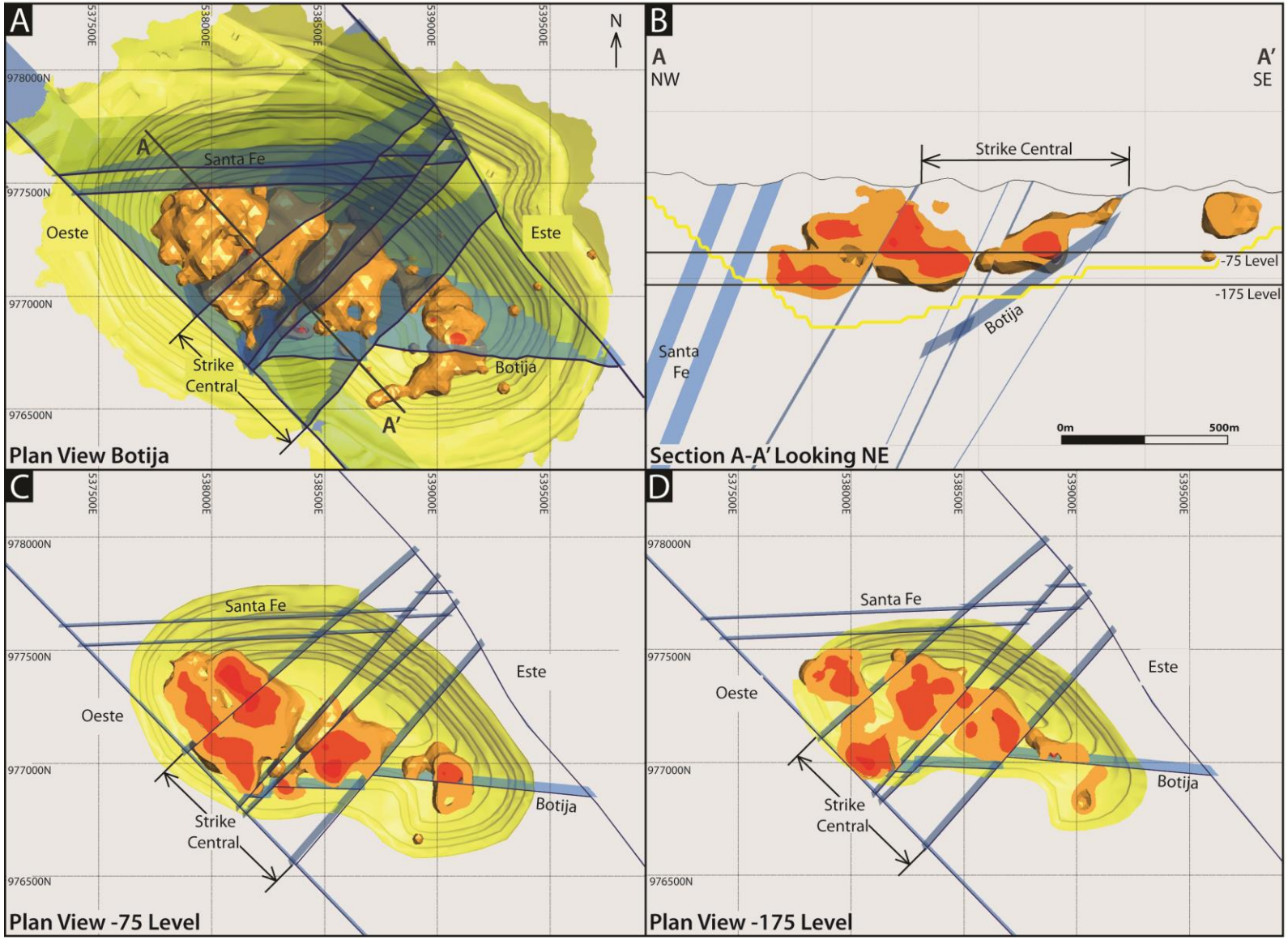
A
537500E
538000E
538500E
539000E
539500E
N
978000N
977500N
977000N
976500N
A
Santa Fe
Oeste
Este
Strike
Central
Botija
A'
Plan View Botija
B
A
NW
A'
SE
Strike Central
-75 Level
-175 Level
Botija
Santa
Fe
0m
500m
Section A-A' Looking NE
C
Santa Fe
Este
Oeste
Botija
Strike
Central
Plan View -75 Level
D
Santa Fe
Este
Oeste
Botija
Strike
Central
Plan View -175 Level

Figure 16: Three dimensional model of 0.5-0.7 wt.% Cu (orange) and >0.7 wt.% Cu (red) and identified fault/fault zones (blue) in the Botija deposit. Modelling was completed in Leapfrog Geo v. 3.1; faults are modelled as hard boundaries in the copper model. The Oeste and Este faults were use as model boundaries, therefore the crosscutting relationship between the northwest striking and Strike Central faults is not included. A. Unclipped plan view of the deposit (looking down) showing the location of major fault zones in relation to the ore body. B. Cross-section A-A' looking NE showing the discontinuity of ore across the Strike Central fault zone. C. Plan view of the -75 m level approximately 200 m below surface. The majority of high grade ore at this level is hosted within or in the hanging wall of the Strike Central fault zone with little high grade material in the foot wall of the Strike Central fault zone. D. Plan view of the -175 m level approximately 300 m below surface. High grade ore is less continuous on this level compared to the -75 m level, with the majority hosted within the Strike Central fault. The Oeste sharply truncates the ore zone on the southwest on this level as well.

A ZTEM™ survey was completed over the Cobre Panamá mining camp in 2010; a processed two-dimensional inversion of this survey was provided for this study (M. Hope, pers. com., 2016). Modelled resistivity values Ohm meters (Ωm) were provided on a 150 m three-dimensional grid covering the Cobre Panamá mining camp, these data were modelled in Leapfrog Geo v. 3.1. Figure 17 is a plan view of the ZTEM™ model and three northwest to southeast cross sections constructed through Balboa, Colina – Valle Grande, and Botija – Botija Abajo. The copper porphyry deposits in the district are associated with low resistance anomalies, with the exception of Botija-Abajo and Brazo, these anomalies are hosted within rocks with distinctly higher resistance. Low resistivity of the deposits is likely related to conductive, sulfide-rich ores. In plan view changes in resistivity can be observed along northwest-southeast corridor that also bounds the extents of several of the deposits. At depth thee cross sections illustrates that these linear ZTEM features dip 30-35°NW and bound the low resistivity anomalies associated with the porphyry deposits. These features are interpreted to be district scale faults in the same strike orientation to the Strike Central fault zone. The 30-35° NW dip of these inferred faults is much less than the ~60°NW dip of the Strike Central fault zone, however, drill core measurements from Botija do support the existence of low angle faults. While compelling field or drill core evidence

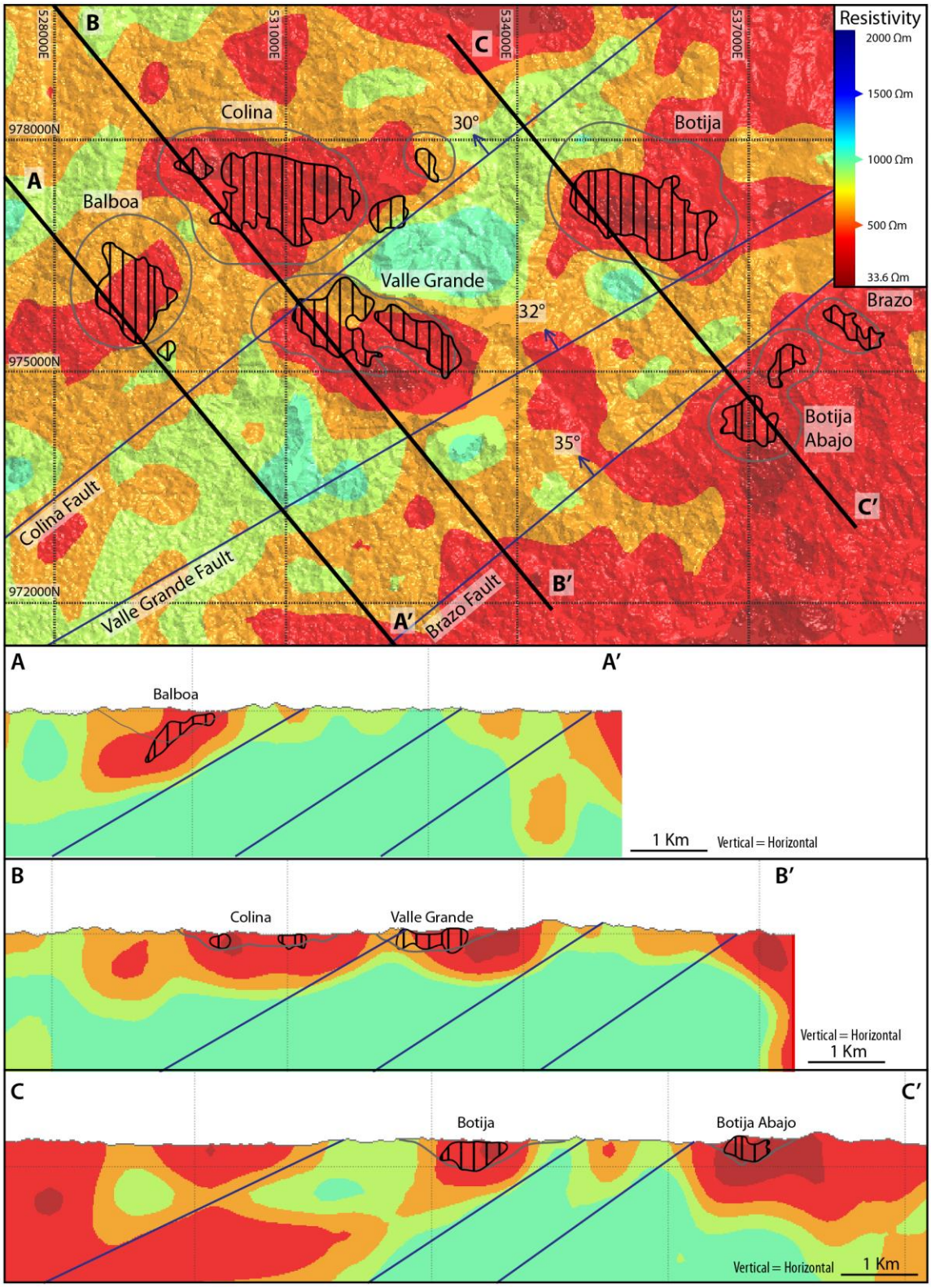

Figure 17: Three dimensional Leapfrog Geo model of ZTEM™ survey of Cobre Panamá mining camp with three cross sections through Balboa (A-A'), Colina-Valle Grande (B-B'), and Botija-Botija Abajo (C-C)'. Ultimate pit limit for the seven deposits is shown in grey and the limit of 0.3 wt.% Cu deposit is shown in black hatch. Faults identified from ZTEM to bound the low resistivity anomalies associated with the deposits are shown in blue.

does not exist for these faults at Botija, the planar nature of the geophysical anomalies, and the presence of some small scale low angle faults in drill core provide evidence for the existence of low angle faults in the district. Rather, the chief fault dipping 30-35° NW inferred from the ZTEM™ data lies southeast of the Botija deposit in an area of poor exposure and little drill data

DISCUSSION

Vertical Zonation of the Botija Deposit:

From petrographic study of the veins and alteration at Botija, it is evident the deposit exhibits many of the classical features of a porphyry copper system with copper introduction associated with high temperature K-silicate alteration and quartz veins. This mineralized high temperature zone is flanked outward and upward by phyllic alteration formed as the magmatic-hydrothermal fluids temporally evolved to cooler and more acidic conditions (Seedorff et al., 2005). The vertical zonation of hydrothermal alteration upward from high to low temperature at Botija occurs over a significantly smaller distance than classical porphyry copper deposits (i.e. El Salvador, Bingham Canyon, Butte, Ann-Mason). Most classical porphyry copper deposits have ore zones with K-silicate alteration which extend >1000 m vertically and have ratios of horizionatl to vertical dimensions that are 1:1 (Butte) or greater (Bingham Canyon or Ann-Mason) (Dilles and Einaudi, 1992; Rusk et al., 2008; Gruen et al., 2010; Redmond and Einaudi, 2010; Houston and Dilles, 2013). At Botija the zonation from high to low temperature alteration occurs over hundreds of meters and the horizontal extent of the deposit is approximately 2000 x 1500 m, which yields a vertical to horizontal ratio of 1:2 to >1:3. These dimensions suggests that the deposit has either been strongly extended and normally faulted similarly to the Robinson deposit (Seedorff et al., 1996; Maher and Seedorff, 2000).

Proposed Reconstruction of Botija:

A three dimensional model of copper, molybdenum, and gold was created using Leapfrog Geo v3.1 using the fault zones identified from logging and mapping to constrain metal distribution. A proposed partial restoration of the three-dimensional copper model is created along cross section D-D' which is perpendicular to the Strike Central fault zone and faults inferred from ZTEM (Figure 18). A restoration of 500 m left-lateral oblique normal displacement was first applied to the Botija fault zone that juxtaposes the barren high temperature K-silicate alteration and quartz veins below the mineralized AB veins while still maintaining an ore shell continuity. By subsequently restoring approximately 500m of normal displacement across the Strike Central fault zone, the ore zone restores partially into the characteristic inverted tea cup shape shaped geometry typical of many copper porphyry deposits (Lowell and Guilbert, 1970; Carten, et al., 1988; Dilles et al., 1992; Tosdal and Richards, 2001; Seedorff et al., 2005; Redmond and Einaudi, 2010; Houston and Dilles, 2013). The net extension from this restoration is oriented approximately ~330-150° northwest-southeast, roughly perpendicular to the rotation axis (Figure 19), as expected for normal faulting (Davis and Reynolds, 1996). This restoration approximates a minimum of 1200 m of original vertical extent to the deposit, yielding a vertical to horizontal dimensions of 1:1 or greater which are more typical dimensions for a porphyry copper deposit. This restoration indicates that additional pieces of the original ore body are missing. Copper mineralization is sharply truncated against the Santa Fe fault zone, shown in black in Figure 18.

This reconstruction also suggests the western limb of the Botija deposit is missing because the NW striking Oeste fault truncates >0.3 wt.% Cu ores and hydrothermal alteration zones on the southeast (Figure 12, Figure, 14). This would require the northwest fault to have normally

offset the orebody significantly, in excess of 250 m, to juxtapose mineralized quartz veins with K-silicate alteration against barren k-silicate alteration with no quartz veins, and potentially a component of left-slip displacement.

While it appears that D veins are down-dropped to the north by the Santa Fe fault on the 538100E section (Figure 14), swarms of aplite dikes observed in drill hole B12163-HG (see Figure 12 for location) north of the Santa Fe fault suggests the hanging wall block of the fault is a deep portion of the hydrothermal system. The presence of D veins in deep of the exposures of the hydrothermal system can also be explained by telescoping of alteration as late fluids are progressively sourced from deeper levels of the magma chamber causing the magmatic fluid plume to migrate downwards, and lower temperature alteration to extend deeper. This process is observed in many deposits including El Salvador, Butte, Bajo De la Alumbrera, and Butte (Gustafson and Hunt, 1975; Meyer, 1967; Proffett, 2003). Additional evidence is provided by deep penetration of D veins into K-silicate alteration in the foot wall of the Oeste fault. While the foot wall of the fault generally contains <0.1 vol.% of D veins, swarms of lode D veins are observed in the foot wall of Oeste fault (Figure 13), these zones average 40 m in width and contain dense swarms of between 0.5 – 16.7 vol.%. These lode veins are generally absent from hanging wall of the Oeste fault and occur only in drill hole B14046 in section 538900E (Figure 15). The elevated arsenic, bismuth, and silver in these veins relative to background are indicative of a higher level style of alteration which has been superimposed on deep K-silicate alteration.

This restoration creates a partially restored ore shell which plunges 50°NE, which is an uncommon angle for a porphyry copper deposit to be emplaced. The quartz and D vein orientations suggest the orebody has been rotated ~40° SW about an axis striking southwest to

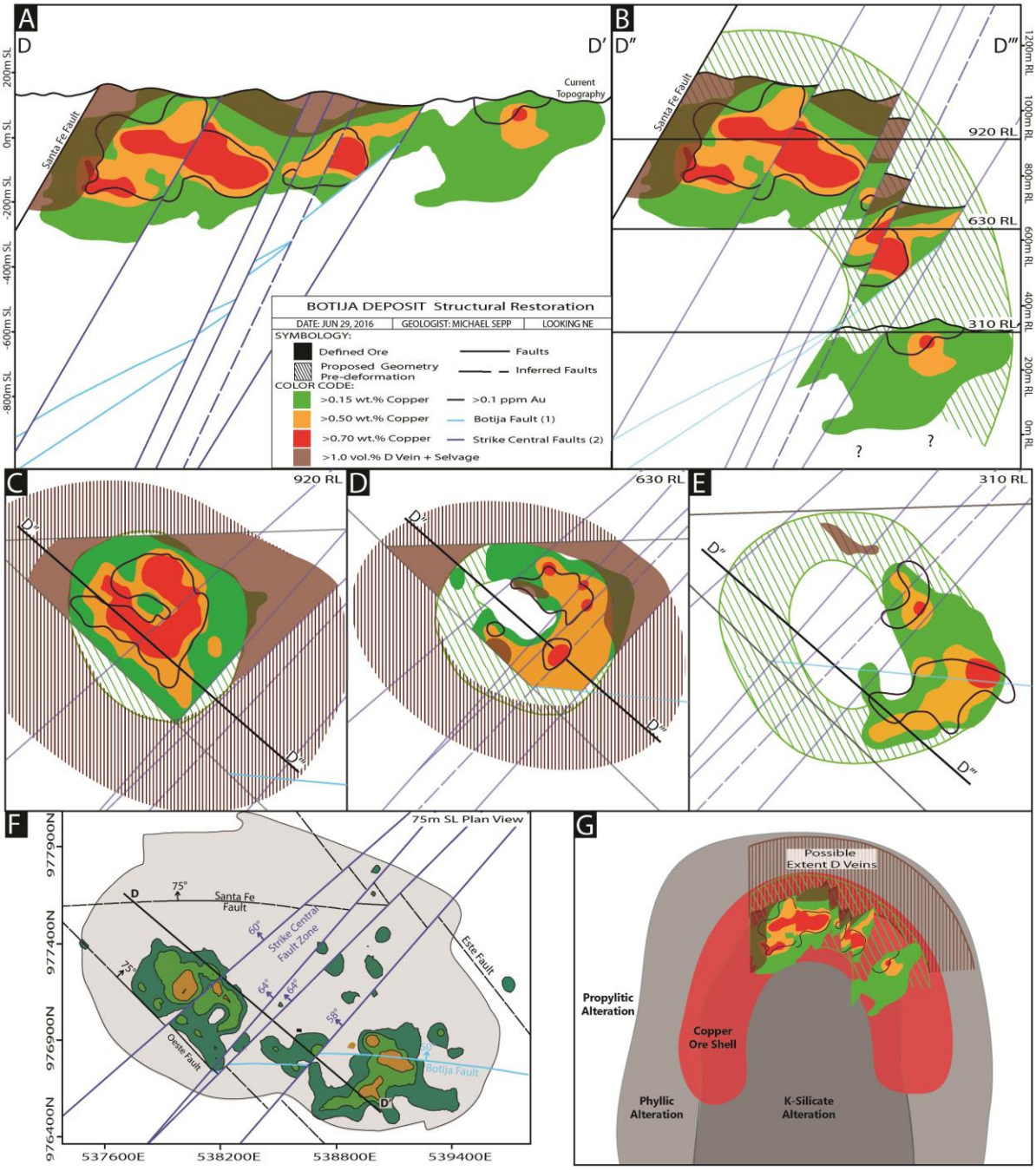

Figure 18: Proposed restoration of the Botija deposit. A. Cross section D-D' on (sea level datum; SL) looking northeast through the Botija deposit showing copper, and gold concentration in addition to the limit of >1.0 vol% D veins inferred from the limit of >3.0 vol% pyrite determined from drill core geochemistry (Helley pers. com., 2015). B. Restoration of the deposit using 500 m of total displacement along the Strike Central fault zone and 500 m oblique normal displacement on the Botija fault zone. Relative elevation (RL) for the reconstruction is provided on the right of the reconstruction. No block rotation is shown, but is inferred to be ~10-15° NW related to these faults. C. Restored plan view of 920 RL with copper, molybdenum, and >1.0 vol% D veins contoured as above, theorized original limits of the hydrothermal footprint are shaded. D. Restored plan view of 630 RL constructed similar to 920 RL. E. Restored plan view of 310 RL with copper, molybdenum, and >1.0 vol% D veins contoured as above, theorized original limits of the hydrothermal footprint are shaded. F. Plan view of the 3D copper concentration contoured model at 75m SL for the current geometry of the Botija deposit with the location of the D-D' cross section restoration. G. Cartoon of tilt restored model (40°SE tilting removed) of the Botija deposit against a simplified copper porphyry model from Lowell and Guilbert (1970).

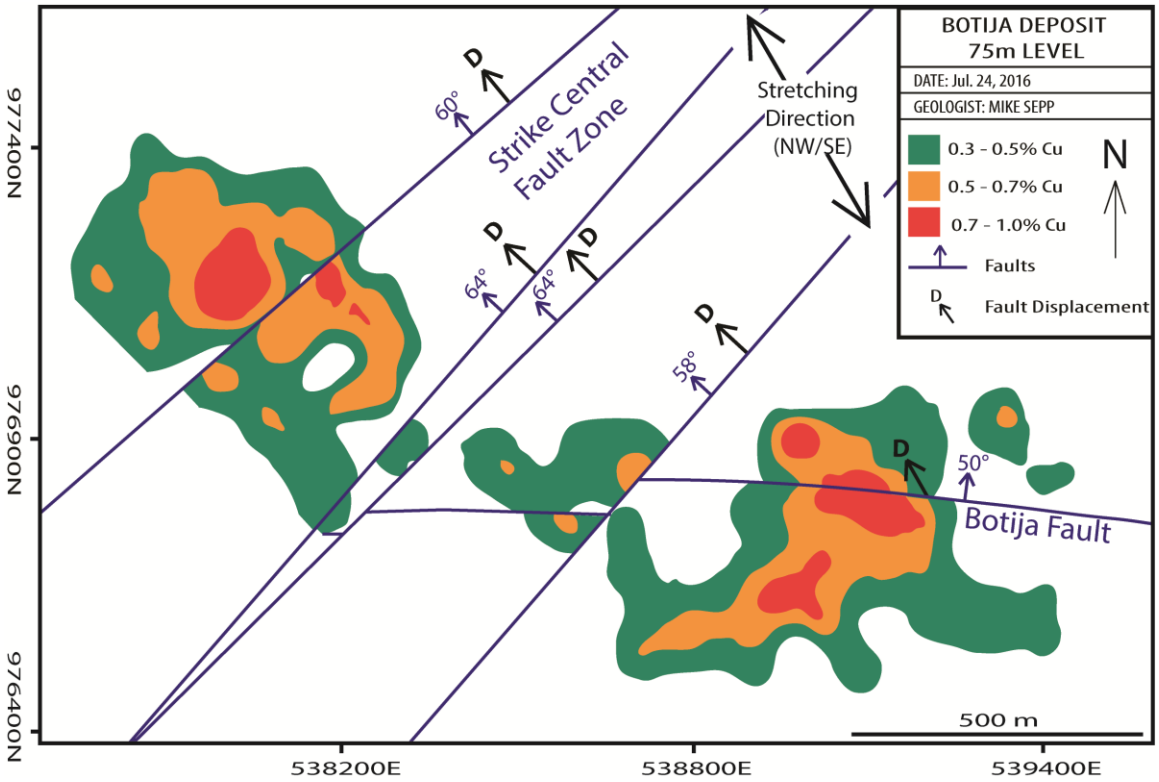

Figure 19: Plan map of the Botija deposit at 75 m elevation (about 50 m below surface) with copper grades contoured and interpreted locations of Botija and Strike Central faults plotted in blue, fault displacements for each fault strand are shown in black. Net extension from the Botija and Strike Central fault zones are oriented on a ~330-150° northwest-southeast trend, extending copper ores to the northwest.

northeast. If a 40°NW rotation about a tilt axes of 240° SW is applied to the quartz and D veins, then all veins restore sub-vertically, and the ore shell restores to a vertical orientation.This rotation angle cannot be explained by identified faults in the Botija ore body itself, which in the restoration appear to tilt the deposit by no more than 10-15°SE. The gently northeast-dipping faults inferred from the ZTEM™ survey are a potential explanation for the additional ~25-30° of SW rotation of the veins and ore shell. Extension in a 330/150° NW/SE orientation would result in normal displacement on these faults, continued extension would lead to block rotation tilting old fault to a flat dipping orientation (Proffett, 1977). Indeed, if a 40°NW tilt restoration is applied to these gently NE dipping faults their dips would restore to 70-75°NW, a range of angles

expected for normal faults. A model of progressive deformation is envisaged, where continued extension rotates early faults which are subsequently cross cut by younger faults (i.e. Strike Central fault zone). This model for faulting at Botija is similar to deposits of the American southwest, where Basin and Range extension has dismembered and extended, several porphyry copper deposits (Proffett, 1977; Seedorff et al., 1991; Seedorff et al., 1996; Maher, 2008; Stavast et al., 2008).

Implications for the Cobre Panamá Mining Camp:

Observations of the orientation, kinematics, and timing of faults at Botija provide insight into the district scale structures at the Cobre Panamá mining camp. The lack of surface exposure of the large regional fault prevents robust geologic constraint of these faults however, geophysical (aeromagnetics) or geomorphic methods (LIDAR) provide some insight into the orientation and kinematics of these fault in conjunction with observations from Botija. The northwest-striking Petaquilla and Medio faults (Figure 2) identified by ZTEM™ aerial magnetics and the orientation of the major rivers are crosscut and offset by southwest striking faults. Though north dipping faults (Botija and Santa Fe) are important at Botija, regional faults similar to the southwest and northeast striking faults are not observed in geophysics or geomorphic datasets. This is likely due to the age of these faults, predating both NW and SW oriented faults causing their geophysical and geomorphic expression to be subdued on large scales.

Copper mineralization at Botija-Abajo and Brazo are associated with advanced argillic pyrophyllite and dickite alteration, in contrast to the deeper K-Silicate alteration associated copper in Botija (C. Burge pers. com., 2015). Soil grid geochemistry also shows arsenic anomalies are associated with the Botija-Abajo and Brazo deposits, whereas the Botija deposit does not

have an enrichment in arsenic. Halley et al. (2015) has demonstrated that arsenic anomalies are characteristic of high level alteration in porphyry copper systems, typically associated with sericitic and advanced argillic alteration, above the higher temperature K-silicate alteration. The high level advanced argillic alteration at Botija-Abajo and Brazo in addition to the low-sulfidation gold mineralization at Mollejón indicates the foot wall of the Brazo fault contains the high level portions of a magmatic hydrothermal system, while the hanging wall contains several deeper K-silicate associated porphyry copper deposits. The area southeast of the Bazo fault therefore appears to be a down dropped possibly by a northeast striking and southeast dipping fault. Indeed, the presence of oppositely dipping normal faults is common in extensional terrains (Davis and Reynolds, 1996).

Integrating district and deposit scale observations, a district scale structural geologic history can be inferred (Figure 20). While it cannot be certain how many porphyry copper centers were originally present in the district, there were likely at least two or three magmatic-hydrothermal centers based on the number of currently identified deposits and locations of post-mineral faults. North-dipping faults, (i.e. Botija and Santa Fe) while important to ore displacement, at a deposit scale are the least continuous faults in the district, indicating they occurred very early in the structural history of the district. Post-dating these east-west faults, normal displacement on northwest-southeast striking faults occurred throughout the district. These faults have been identified to be orientated 320/75°NE at the Botija deposit, however, in the Colina deposit previous studies have constrained these faults to be orientated strike 157°SE and dip 30-45°SW (Nobel and Benavides 2013; 2014; Speidel and Faure, 1996). If the same 40°NW rotation is applied to the northwest-southeast striking faults at Botija and Colina, as proposed based on

veins at Botija, the dips of these faults restore 50°SE (Santa Fe) and 90°NE (Botija), dips expected for normal faults. The latest generation of faults have northeast-southwest strike and was responsible for the block rotation, dismembering and rotating the deposits into their current geometry.

Based on this restoration it is proposed that northwest-southeast striking faults and southwest striking faults are responsible for the majority of normal displacement of mineralization at a district scale. Early studies have suggested these fault sets occurred as conjugate sets, however, the discontinuity of northwest-southeast striking faults in magnetic and ZTEM surveys, and the associated jogs in rivers which follow these faults by northeast-southwest faults indicates these faults moved earlier than northeast-southwest striking faults.

Over the geologic history of Panamá, strike-slip faults have been identified as the dominate form of deformation (Lissinna, 2005; Kerr and Tarney, 2005; Bennett et al., 2014; Trendkam et al., 2002). Work by Farris et al. (2011) suggested that localized normal faulting occurred in Panamá in response to the development of the Panamá orocline (Farris et al., 2011; Silver et al., 1990). This interpretation of dominant normal faulting in the Cobre Panamá mining camp is consistent with the thermochronology by Farris et al. (2011) which suggest the exhumation of the Botija deposit occurred during a period of extension in portions of Panamá between 19.5 – 22.3 Ma.

This model is simplistic due to the limited amount of field studies and poor field exposures and therefore robust data are not available to confirm the hypotheses by previous studies that thrust and strike slip fault motion has been important in the district. Indeed, it is likely given the

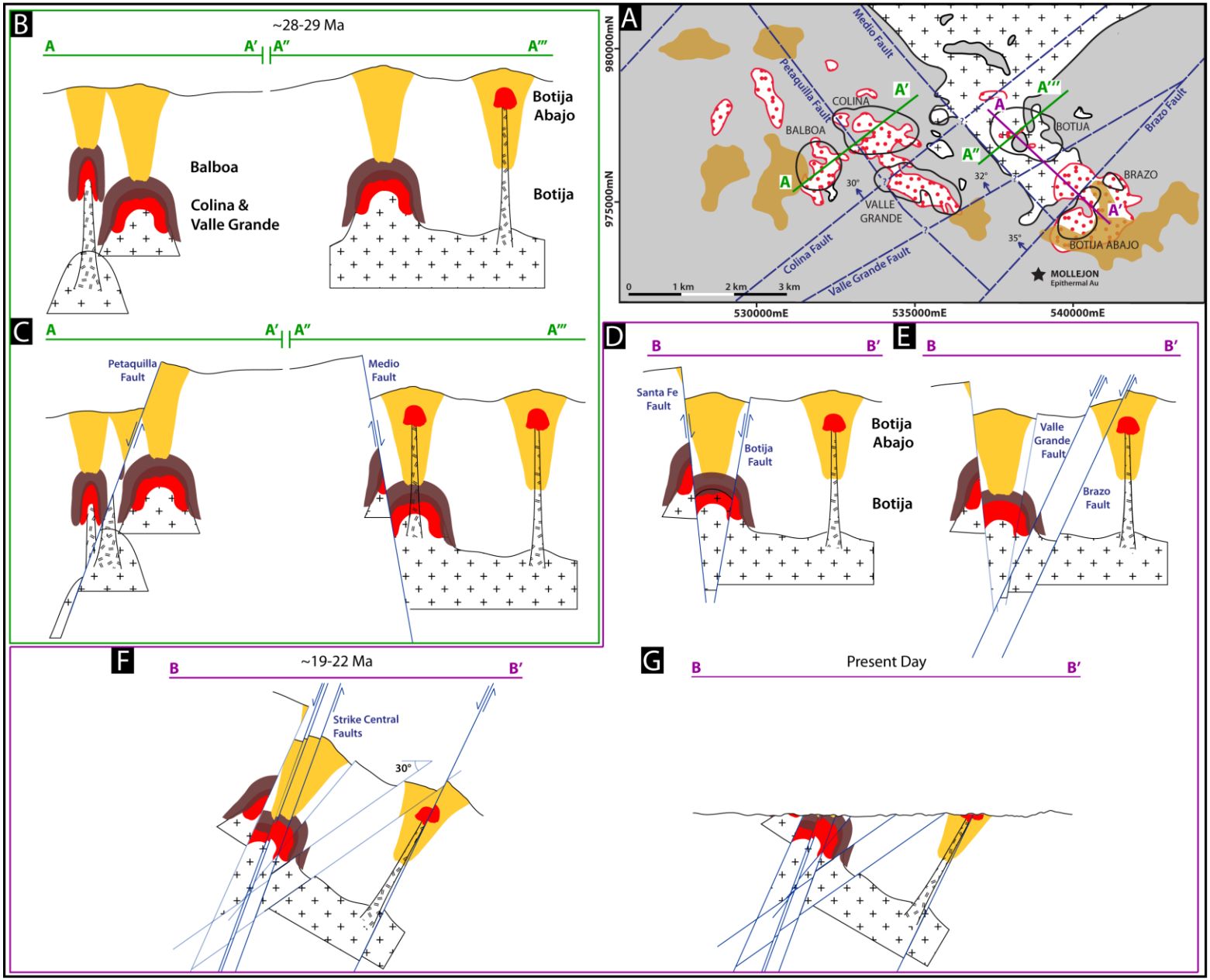
A
980000mN
975000mN
Medio Fault
Petaquilla Fault
COLINA
BALBOA
A'
A''
A'''
A
BOTIJA
Brazo Fault
30°
32°
BRAZO
VALLE
GRANDE
35°
BOTIJA ABAJO
Colina Fault
Valle Grande Fault
MOLLEJON
Epithermal Au
0
1 km
2 km
3 km
530000mE
535000mE
540000mE
B
~28-29 Ma
A
A'
A''
A'''
Botija
Abajo
Balboa
Botija
Colina &
Valle Grande
C
A
A'
A''
A'''
Petaquilla
Fault
Medio
Fault
D
B
B'
Santa Fe
Fault
Botija
Fault
Botija
Abajo
Botija
E
B
B'
Valle
Grande
Fault
Brazo
Fault
F
B
~19-22 Ma
B'
Strike Central
Faults
30°
G
B
Present Day
B'

Figure 20: Cartoon of proposed northwest-southeast and northeast-southwest faulting in the Cobre Panamá mining camp, age dates constraining the emplacement of (A) and exhumation of (B) the deposits are shown at their respective time steps (Farris et al., 2011; Baker et al., 2016). Parts A and B illustrate northwest-southeast faulting through all the deposits, while C - F show northeast-southwest faulting through Botija, Botija-Abajo, and Brazo A. Emplacement of Porphyry copper deposits B. Normal displacement on northwest-southeast faults C. Normal faulting on east-west striking faults on the Botija and Botija-Abajo. D. Normal Faulting on southwest striking fault down dropping Botija. E. Continued extension and block rotation, formation of smaller scale normal faults (Strike Central fault zone) dismembering Botija deposit. F. Erosion to present level.

long lived deformation history of Panamá that additional structural events have occurred. As noted above it is possible that normal-oblique displacement could have occurred on many of these faults, however, due to the lack of identifiable marker bed stratigraphy or intrusive contacts, absolute fault displacement amounts are difficult to constrain with the currently available dataset. Nonetheless, the restorations of the magmatic hydrothermal systems indicate that normal faulting has been the dominate form of displacement on the faults which cut through the Cobre Panamá mining camp.

CONCLUSIONS

The petrography and geochemistry of the rocks at Botija indicate the deposit has evolved through a classic magmatic-hydrothermal progression characteristic of porphyry copper systems. The strong horizontal elongation of the hydrothermal footprint indicates the deposit has been strongly deformed subsequent to emplacement, and the mapped and inferred normal displacements along faults suggests that normal faulting produced most of the deformation. Net extension on the order of approximately 1000 m can be estimated on west and southwest striking faults in Botija, and restoration of this displacement partially brings the orebody into an inverted ‘tea cup’ geometry characteristic of porphyry deposits. The recognition of post-mineralization extension at Botija is consistent with the results by Farris et al. (2011) that constrained the

exhumation of the deposit to a period of localized extension in the Miocene (19.5 – 22.3 Ma) Panamá related to oroclinal bending of the volcanic arcs.

This reconstruction indicates that part of the original orebody are missing due to a combination of fault displacement and erosion at Botija. Figure 18c-e shows that mineralization in the foot wall of the Oeste fault and hanging wall of the Santa Fe fault are presently not accounted for with the current drill core data. Lateral motion with a dip-slip component on the Oeste fault could have offset the southwest portion of the original ore shell, moving it to the northwest or southeast from the Botija deposit (Figure 12). Additional mineralization associated with advanced argillic alteration and inferred to be the upper parts of the Botija and Botija Abajo magmatic-hydrothermal systems has also likely been extended in the area between the Botija and Botija-Abajo deposits by the southwest striking Colina and Valle Grande faults (Figure 17).

This reconstruction also has implications on the development of the other deposits in the district, and to exploration potential for other orebodies. Northwest- and southwest-striking faults inferred from regional geophysical surveys (aeromagnetics and ZTEM™) have, the same orientation as the Oeste and other faults at the Botija deposit, and also bound or offset several of the other copper porphyry deposits in the area (Figure 2). These observations suggest that the other deposits of the Cobre Panamá mining camp have likely been dismembered similarly to the Botija deposit. Additional limbs of porphyry copper mineralization from other presently identified deposits have likely also been extended along northwest-southeast axes. This elongation of mineralization increases the prospectivity for future near mine exploration to identify additional resources in close proximity to already planned mine infrastructure.

REFERENCES

Baker, M.J., Hollings, P., Thompson, J.A., Thompson, J.M., and Burge, C., 2016, Age and geochemistry of host rocks of the Cobre Panamá porphyry Cu-Au deposit, central Panamá: Implications for the Paleogene evolution of the Panamánian magmatic arc: Lithos, v. 248-251, p. 40-54.

Birch, C., 2014, New systems for geological modelling-black box or best practice?: Journal of the Southern African Institute of Mining and Metallurgy, v. 114, p. 993-1000.

Bryan, J.R., 2013, Biostratigraphic report on larger foraminifera from the Panamá core sample from Cobre Panamá: Unpublished Report, p. 1-2.

Burke, K., Fox, P.J., and Sengör, M.C., 1978, Buoyant Ocean Floor and the Evolution of the Caribbean: Journal of Geophysical Research, v. 83, p. 3949-3954

Burnham, C.W., 1979, Magmas and hydrothermal fluids: Barnes, H.L. ed., Geochemistry of hydrothermal ore deposits: New York, Wiley Intersci., p. 71-136.

Carr, J.C., Beatson, R.K., Cherrie, J.B., Mitchell, T.J., Fright, W.R., McCallum, B.C., and Evans, T.R., 2001, Reconstruction and representation of 3D objects with radial basis functions: In Proceedings of the 28th annual conference on Computer graphics and interactive techniques, p. 69-76.

Carten, R.B., Geraghty, E.P., Walker, B.M., and Shannon, J.R., 1988, Cyclic development of igneous features and their relationship to high-temperature hydrothermal features in the Henderson porpoyry molybdenum deposit, Colorado: Economic Geology, v. 83, p. 266-296.

Cowan, E.J., Beatson, R.K., Fright, W.R., McLennan, T.J., and Mitchell, T.J., 2002, Rapid geological modelling: Applied Structural Geology for Mineral Exploration and Mining, International Symposium.

Davis, G.H., Reynolds, S.J., 1996, Structural geology of rocks and regions: John Wiley & Sons, INC. p. 150-202.

Dilles, J.H., 1987, Petrology of the Yerington Batholith, Nevada: Evidence for Evolution of Porphyry Copper Ore Fluids: Economic Geology, v. 82, p. 1750-1789.

Dilles, J.H., and Einaudi, M.T., 1992, Wall-Rock Alteration and Hydrothermal Flow Paths above the Ann-Mason Porphyry Copper Deposit, Nevada – A 6-Km Vertical Reconstruction: Economic Geology, v. 87, p. 1963-2001.

Drummond, M.S., Bordelon, M., De Boer, J.Z., Defant, M.J., Bellon, H., and Feigenson, M.D., 1995, Igneous petrogenesis and tectonic setting of plutonic and volcanic rocks or the cordillera de talamanca, Costa Rica – Panamá, central American arc: American Journal of Science, v. 295, p. 875-919.

Einaudi, M.T., 1997, Mapping altered and mineralized rocks: The “Anaconda Method”: Unpublished short-course notes.

Farris, D.W., Jaramillo, C., Bayona, G., Restrepo-Moreno, S.A., Montes, C., Cardona, A., Mora, A., Speakman, R.J., Glascock, M.D., and Valencia, V., 2011, Fracturingof the Panamánian Isthmus during initial collision with South America: Geology, v. 39, p. 1007-1010.

Cernuschi, F., 2015, The Geology and Geochemistry of the Haquira East Porphyry Copper Deposit of Southern Peru: Insights on the Timing, Temperature and Lifespan of the Magmatic-hydrothermal Alteration and Mineralization: Phd Dissertation Oregon State University, p. 1-283.

Gazel, E., Hoernle, K., Carr, M.J., Herzberg, C.C., Saginor, I., van den Bogaard, P., Hauff, F., Feigenson, M., and Swisher III, C., 2011, Plume-subduction interaction in southern Central America: Mantle upwelling and slab melting: Lithos, v. 121, p. 117-134.

Gazel, E., Carr, M.J., Hoernle, K., Feigenson, M.D., Szymanski, D., Hauff, F., and van den Bogaard, P., 2009, Galapagos-OIB signature in southern Central America: Mantle refertilization by arc-hot spot interaction: Geochemistry, Geophysics, Geosystems: v. 10(2).

Grey, D., Lawlor, M., and Stone, R., 2015, Cobre Panamá Project Colon Province, Republic of Panamá NI

43-101 Technical Report: NI 43-101 Technical Report, p. 40-58.
Gruen, G., Heinrich, C.A., Schroeder, and K., 2010, The Bingham Canyon Porphyry Cu-Mo-Au Deposit. II. Vein Geometry and Ore Shell Formation by Pressure-Driven Rock Extension: Economic Geology, v. 105, p. 69-90.
Gustafson, L.B. and Hunt, J.P., 1975, The porphyry copper deposit at El Salvador, Chile: Economic Geology, v. 70, p. 857–912.
Gustafson, L.B. and Quiroga, J., 1995, Patterns of Mineralization and Alteration below the Porphyry Copper Orebody at El Salvador, Chile: Economic Geology, v. 90, p. 2-16.
Halley, S., 2014, The geochemistry and Mineralogy of Botija Deposit, Unpublished presentation for FQM, p. 1-85.
Halley, S., Dilles, J.H., and Tosdal, R.M., 2015, Footprints: Hydrothermal Alteration and Geochemical Dispersion Around Porphyry Copper Deposits: SEG Newsletter, v. 100, p. 12-17.
Hardy, R.L., 1971, Multiquadric equation of topography and other irregular surfaces: Journal of Geophysical Research, v. 76, p. 1905-1915.
Hoernle, K., Hauff, F., and van den Bogaard, P., 2004, 70 m.y. history (139-69 Ma) for the Caribbean large igneous province: Geology, v. 32, p. 697-700.
Hoernle, K., van den Bogaard, P., Werner, R., Lissinna, B., Folkmar, H., Alvarado, G., and Garbe-Schönberg, D., 2002, Missing history (16-71 Ma) of the Galápagos hotspot: Implications for the tectonic and biological evolution of the Americas: Geology, v. 30, p. 795-798.
Heidrick, T.L., and Titley, S.R., 1982, Fracture and dike patterns in Laramide plutons and their structural and tectonic implications: American southwest, *in* Titley, S.R. ed., Advances in geology of the porphyry copper deposits: Tucson, University of Arizona Press, p. 73-91.
Houston, R.A. and Dilles, J.H., 2013, Structural Geologic Evolution of the Butte District, Montana: Economic Geology, v. 108, p. 1397-1424.
Kerr, A.C., and Tarney, J., 2005, Tectonic evolution of the Caribbean and northwestern South America: The case for accretion of two Late Cretaceous oceanic plateaus: Geology, v. 33, p. 269-272.
Kesler, S.E., Sutter, J.F., Issigonis, M.J., Jones, L.M., and Walker, R.L., 1977, Evolution of Porphyry Copper Mineralization in an Oceanic Island Arc: Panamá: Economic Geology, v. 72, p. 1142-1153.
Legault, J.M., Kaminski, V., Kumar, H., Orta, M., and Prikhodko, A., 2010, Helicopter Clectromagnetic (VTEM and ZTEM Applications for Gold Exploration: KEGS-PDAC Symposium.
Lissinna, B., 2005, A profile through the Central American Landbridge in western Panamá: 115 Ma Interplay between the Galapagos Hotspot and the Central American Subduction Zone: Phd Dissertation Christian-Albrechts – University Keel, p. 1-115.
Loewen, M.W., Duncan, R.A., Kent, A.J., and Krawl, K., 2013, Prollonged plume volcanism in the Caribbean Large Igneous Province: new insights from Curaçao and Haiti: Geochemistry, Geophysics, Geosystems, v. 14, p. 4241-4259.
Lowell, J.D., and Guilbert, J.M., 1970, Lateral and vertical alteration-mineralization zoning in porphyry ore deposits: Economic Geology, v. 65, p. 373-408.
Maher, D.J., 2008, Reconstruction of Middle Tertiary Extension and Laramide Porphyry Copper Systems, East Central Airizona: Phd Dissertation University of Airizona
Maher, D.J., and Seedorff E., 2000, Post-mineral structure of the Liberty area, Robinson (Ely) porphyry copper deposit, White Pine County, Nevada [abs]: Geological Society of America Abstracts with Programs, v. 32, p. A232-A233.
Meyer, C., 1965, An early potassic type of alteration at Butte, Montana: American Mineralogist, v. 50, p. 1717-1722.
Meyer, C., and Hemley, J.J., 1967, Wall rock alteration: Geochemistry of hydrothermal ore deposits, v. 1, p. 166.
Montero, W., Denyer, P., Barquero, R., Alvarado, G.E., Cowan, H., Machette, M.N., Haller, K.M., and

Darth, R.L., 1998, Map and database of Quaternary faults and folds in Costa Rica and its offshore regions: US Geological Survey Open File Report, v. 98-481, p. 1-63.
Nobel, M., and Benavides, S., 2013, Cobre Panamá Mapping 2013: Unpublished report by Model Earth for First Quantum Minerals, p. 1-25.
Nobel, M., and Benavides, S., 2014, Cobre Panamá Mapping 2014 – Colina and Medio Deposits: Unpublished report by Model Earth for First Quantum Minerals, p. 1-21.
Paris, G., Machette, M.N., Dart, R.L., Haller, K.M., 2000, Map and database of Quaternary faults and folds in Columbia and its offshore regions: US Geological Survey Open File Report, v. 00-0284, p. 1-60.
Pirajno, F., 2009, Hydrothermal Processes and Mineral Systems: Springer Science, p. 90-97
Proffett, J.M., 1973, Structure of the Butte district, Montana: A field meeting held in August, p. 18-21.
Proffett, J.M., 1977, Cenozoic geology of the Yerington district, Nevada ,and its implications for the nature and origin of Basin and Range faulting: Geological Society of America Bulletin, v. 88, p. 247-266.
Proffett, J.M., 2003, Geology of the Bajo de la Alumbrera Porphyry Copper-Gold Deposit, Argentina: Economic Geology, v. 98, p. 1535-1574.
Redmond, P.B. and Einaudi, M.T., 2010, The Bingham Canyon Porphyry Cu-Mo-Au Deposit. I. Sequence of Intrusions, Vein Formation, and Sulfide Deposition.
Rockwell, T.K., Bennett, R.A., Gath, E., and Franceschi, P., 2010a, Unhinging an indenter: A new tectonic model for the internal deformation of Panamá: Tectonics, v.29(4)
Rockwell, T.K., Gath, E., González, T., Madden, C., Verdugo, D., Lippincott, C., Dawson, T., Owen, L.A.,
Fuchs, M., Cadena, A., Williams, P., Weldon, E., and Franceschi, P., 2010b, Neotectonics and Paleoseismology of the Limón and Pedro Miguel Faults in Panamá: Earthquake Hazard to the Panamá Canal: Bulletin of the Seismological Society of America, v. 100, p. 3097-3129.
Rooney, T.O., Franceschi, P., and Hall, C.M., 2011, Water-saturated magmas in the Panamá Canal region: a precursor to adakite-like magma generation?: Contributions to Mineralogy and Petrology, v. 161, p. 373-388.
Ross, K. and Thompson, A., 1996, PetraScience Consultants Petrography Report Petaquilla Project: Unpublished Report by PetraScience for Inment Mining, p. 8-24.
Rusk, B.G., Reed, M.H., and Dilles, J.H., 2008, Fluid Inclusion Evidence for Magmatic-Hydrothermal Fluid Evolution in the Porphyry Copper-Molybdenum Deposit at Butte, Montana: Economic Geology, v. 103, p. 307-334.
Rutter, H., 2011, Monograph 9 – Field Geologists Manual: AusIMM, p. 323-324.
Sales, R.H., and Meyer, C., 1948, Wall rock alteration at Butte, Montana: Transactions of the American Institute of Mining and Metallurgical Engineers, v. 178, p. 9-35.
Seedorff, E., 1991, Magmatism, extension, and ore deposits of Eocene to Holocene age in the Great Basin--Mutual effects and preliminary proposed genetic relationships, *in* Raines, G. L., Lisle, R. E., Schafer, R. W., and Wilkinson, W. H., eds.: Geology and ore deposits of the Great Basin: Geological Society of Nevada, Symposium, Reno/Sparks, April 1990, Proceedings, v. 1, p. 133-178.
Seedorff, E., Dilles, J.H., Proffett, J.M., Einaudi, M.T., Zurcher, L., Stavast, W.J., Johnson, D.A., and Barton, M.D., 2005, Porphyry Deposits: Characteristics and Origin of Hypogene Features: Economic Geology 100th Anniversary Volume, p. 251-298.
Seedorff, E., Hasler, R.W., Breitrick, R.A., Fahey, P.L., Jeanne, R.A., Shaver, S.A., Stubbe, P., Troutman, T.W., and Manske, S.L., 1996, Overview of the Geology and ore Deposits of the Robinson District, with Emphasis on its Post-Mineral Structure: Geology and ore deposits of the American Cordillera: field trip guidebook compendium, Reno/Sparks, April 1996, p. 81-91.

Segall, P., and Pollard, D.D., 1983, Nucleation and Growth of Strike Slip Faults in Granite: Journal of Geophysical Research, v. 88, p. 555-568.
Sillitoe, R.H., 2010, Porphyry Copper Systems: Economic Geology, v.105, p.3-41.
Silver, E.A., Reed, D.L., Tagudin, J.E., and Heil, D.R., 1990, Implications of the north and south Panamá thrust belts for the origin of the Panamá orocline, Tectonics, v.9, 261-281.
Speidel, F. and Faure, S., 1996, Petaquilla Project, Republic of Panamá Surface Geology Of Botija and Petaquilla Deposits: Unpublished Inmet Report, p. 1-36.
Speidel, F., Faure, S., Smith, M.T., and McArthur, G.F., 2001, Exploration and Discovery at the Petaquilla Copper-Gold Concession, Panamá: Special Publication-Society of Economic Geologist, v. 8, p. 349-362.
Stavast, W.J.A, Butler, R.F., Seedorff, E., Barton, M.D., and Ferguson, C.A, 2008, Tertiary Tilting and Dismemberment of the Laramide Arc and Related Hydrothermal Systems, Sierrita Mountains, Airizona: Economic Geology, v. 103, p. 629-636.
Stewart, M., de Lacey, J., Hodkewics, P.F., and Lane, R., 2014, Grade Estimation from Radial Basis Functions – How does it compare with Conventional Geostatistical Estimation: In Proceedings of the Ninth International Mine Geology Conference, p. 18-80.
Stewart, R.H., and Stewart, J.L., 1980, Geologic map of the Panamá Canal and vicinity, Republic of Panamá: US Geological Survey Open Report, v. 1232.
Titley, S.R., Thompson, R.C., Haynes, F.M., Manske, S., Robison, L.C., and White, J.L., 1986, Evolution of fractures and alteration in the Sierrita-Esperanza hydrothermal system, Pima County, Arizona: ECONOMIC GEOLOGY, v.81, p. 343-370.
Tosdal, R.M., and Richards, J.p., 2001, Magmatic and structural controls on the development of porphyry Cu ± Mo ± Au depsoits: Reviews in Economic Geology, v. 14, p. 157-181.
Villeneuve, M., 1997, Report on 40Ar/39Ar age dates for samples from Petaquilla deposit: Unpublished report by Geological Survey of Canada for Inmet Mining, p. 4.
Vozoff, K., 1972, The magnetotelluric method in the exploration of sedimentary basins: Geophysics, v. 37, p. 98-141.
Wegner, W., Wörner, G., Harmon, R.S., and Jicha, B.R., 2011, Magmatic history and evolution of the Central American Land Bridge in Panamá since Cretaceous times: GSA Bulletin, v. 123, p. 703-724.
Weis, P., Driesner, T., and Heinrich, C.A., 2012, Porphyry-Copper Ore Shells Form at Stable Pressure-Temperature Fronts Within Dynamic Fluids Plumes: Science, v. 338, p. 1613-1616.
Whattam, S.A., Montes, C., McFadden, R.R., Cardona, A., Ramirez, D., and Valencia, V., 2012, Age and origin of earliest adakitic-like magmatism in Panamá: Implications for the tectonic evolution of the Panamánian magmatic arc system: Lithos, v. 142-143, p. 226-244.

APPENDIX

Data for this study has been compiled into to digital volumes on CDs, the contents of each CD is as follows.

Appendix Disk 1:

1. 1_MapData: Scanned map sheets from bench and trench mapping across the Botija deposit.
2. 2_Petrography: Notes on veins and alteration, their paragenesis, and hyperspectral images of selected samples.
3. 3_Geochemistry: Raw data and IoGas files of geochemical suite sent as a part of this study to ALS.
4. 4_CrossSections: Field and office hand interpretations of three cross sections logged.
5. 5_Leapfrog: Leapfrog Geo project file containing the Botija model generated as part of this study.

Appendix Disk 2:

1. 1_MasterDatabase: Digital database of logging data, vein orientation data, geochemistry, sample descriptions, and photographs collected during field work.
2. 2_PaperLogs: Scanned paper diamond drill core logs collected during field work.
3. 3_Legends: Legends of abbreviations used in FQM and by M. Sepp for logging and mapping.